Sedimentary Geology 483 (2025) 106899

Contents lists available at ScienceDirect

Sedimentary Geology

journal homepage: www.elsevier.com/locate/sedgeo

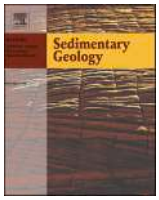

Gastropod-rich lacustrine carbonate deposits in N Iberia: a depositional, climatic and ecological record of the Late Miocene

Zuriñe Larena [a,*], Concha Arenas [b], Josep Sanjuan [c], Ana Pascual [a], Mariano Larraz [d], Xabier Murelaga [a], Juan Ignacio Baceta [a]

[a] Department of Geology, University of the Basque Country (UPV/EHU), 48080 Bilbao, Spain
[b] Department of Earth Sciences, Institute for Research on Environmental Sciences of Aragón (IUCA) and GeoTransfer Group, University of Zaragoza, 12 Pedro Cerbuna St, 50009 Zaragoza, Spain
[c] Departamento de Dinámica de la Tierra y del Océano, Facultad de Ciencias de la Tierra, Martí i Franqués, s/n, E-08028 Barcelona, Spain
[d] Departamento de Biología Ambiental (Zoología), Facultad de Ciencias, Universidad de Navarra, Apartado 177, E-31080, Spain

ARTICLE INFO

Editor: Dr. Catherine Chagué

Keywords:
Carbonate facies
Lacustrine
Palustrine
Freshwater gastropods
Late Miocene

ABSTRACT

The Tortonian Peña Adrian Formation represents the youngest depositional unit of the Miranda-Trebiño basin (Basque-Cantabrian Pyrenees), which developed on the Southern Basque-Cantabrian Pyrenees from late Eocene to Late Miocene times. The formation is a 50–160 m thick succession of alluvial detrital grading to lacustrine carbonates that contain rich and varied calcareous fossil biota (gastropods, ostracods and charophytes). The fossil association characterizes warm temperate, shallow lakes with vegetated bottoms and well-oxygenated and alkaline fresh waters. Integration of stratigraphic, sedimentological, paleontological and C—O stable isotopic data allows the differentiation of a wide range of sedimentary facies, the construction of a depositional model and the definition of distinct evolutionary phases and relation to allogenic processes. Up to 3 metre-thick facies sequences record repetitive water-level changes, likely reflecting short-term climate changes. Overall, the succession outlines an asymmetric cycle of gradual expansion and faster contraction of a shallow ramp-like lake system evolving under oscillating climatic conditions. C and O stable isotopes are consistent with decreasing salinity and increasing precipitation/evaporation balance trough time. Excellent preservation of aragonitic and bimineralic gastropods characterizes the open lacustrine deposits, whereas shell dissolution and neomorphism are distinct in the palustrine ones. This contrasting degree of preservation of calcareous biota clearly reflects changes in the physico-chemical conditions that prevailed during sedimentation and early burial. The findings add to the knowledge of carbonate lake basins, help discern the factors that controlled their evolution and highlight specific depositional and preservation conditions for gastropod-rich carbonate records.

1. Introduction

The study of modern and ancient lacustrine carbonate systems has increased considerably in the last decades, given their high sensitivity to environmental changes at both short and long-term time scales. These non-marine carbonates have demonstrated to be excellent indicators of regional climate, tectonism and depositional conditions and thus can provide key information for palaeogeographical reconstructions and inter-regional correlations of sedimentary and biological evolutionary trends (Kelts and Talbot, 1990; Platt and Wright, 1991; Arenas and Pardo, 1999; Bohacs et al., 2000; Gierlowski-Kordesch, 2010; Vázquez-Urbez et al., 2013; Arenas et al., 2024; Benavente and Bohacs, 2024). The regional geology controls the nature of the catchment and solute-sediment source areas and, additionally, determines several intrinsic features of the lacustrine basins such as topography, geomorphology, subsidence rates, depocentre distribution, their open or closed character and their variation through time (Carroll and Bohacs, 1999; Davis et al., 2008; Platt and Wright, 2024). The regional climate controls the hydrology (i.e., through surface and groundwater recharge) and the temperature, with an impact on the net balance between precipitation and evaporation; in closed-lake basins, the latter parameters can influence in the chemistry of lake waters and the type of lacustrine deposits and

* Corresponding author.
E-mail addresses: zurine.larena@ehu.eus (Z. Larena), carenas@unizar.es (C. Arenas), josepsanjuan@ub.edu (J. Sanjuan), ana.pascual@ehu.eus (A. Pascual), mlarraz@external.unav.es (M. Larraz), xabier.murelaga@ehu.eus (X. Murelaga), juanignacio.baceta@ehu.eus (J.I. Baceta).

https://doi.org/10.1016/j.sedgeo.2025.106899
Received 7 February 2025; Received in revised form 15 May 2025; Accepted 16 May 2025
Available online 20 May 2025

associated biotas (Arenas et al., 2024; Benavente and Bohacs, 2024). Furthermore, climate may exert direct control on cyclical or episodic lake water level variations, which combined with local tectonism may cause marked facies shifts and complex sedimentary stacking patterns involving a wide range of clastic, carbonate and/or evaporitic sediments (Platt and Wright, 1991; De Wet et al., 1998; Alonso-Zarza, 2003; Gierlowski-Kordesch, 2010; Alonso-Zarza et al., 2012).

Lacustrine carbonate successions were common during the Miocene in the Iberian Peninsula, located in the western Mediterranean domain, at similar latitude than today. Carbonate and evaporitic lakes were particularly common and extensive during the Early and Middle Miocene, most likely by the combination of warm subtropical climates (Zachos et al., 2001; Shevenell et al., 2004; Jiménez-Moreno et al., 2010) and the formation of numerous closed or semiclosed foreland and piggy-back basins associated to the Alpidic convergence (Friend and Dabrio, 1996). The global trend to cooler and drier conditions after the Miocene Climatic Optimum (MCO) (Steinthorsdottir et al., 2020) prompted a significant decrease in the extension of the Iberian lacustrine systems. Among the best documented case studies are the carbonate lacustrine to fluvio-lacustrine successions of the Ebro Basin (Arenas and Pardo, 1999; Vázquez-Urbez et al., 2013) and the Madrid Basin (Sanz, 1994; Wright et al., 1997), the Cuestas and Calizas del Páramo lacustrine successions of the Duero and Almazán Basins (Armenteros, 1991; Huerta, 2006), the palustrine to lacustrine deposits of Miocene-Pliocene age in the Teruel basin (Alonso-Zarza et al., 2002; Ezquerro, 2017), and the Upper Miocene carbonate-evaporite successions of the Bicorp Basin (Anadón et al., 1998). One of the most distinctive features of these systems was the development of extensive matrix-rich limestones with moderate to abundant bioclastic content, in some cases associated to evaporites and significant amounts of microbial carbonates (i.e. oncoidal and stromatolitic limestones). However, none of those studies reported a lake context with varied and abundant calcareous biota, in particular well-preserved molluscs, which might indicate specific depositional, hydrological and preservation conditions.

The lacustrine deposits of the Peña Adrian Formation, a Late-Miocene unit of alluvial clastics and lacustrine carbonate deposits exposed on the Miranda-Trebiño piggy-back basin (southern Basque Pyrenees, North Spain), offer a unique resource for a comprehensive analysis of stratigraphic architecture, depositional environment, and paleoecological and paleoclimate implications. The carbonates stand out for a wide array of palustrine and lacustrine deposits, including extensive intervals very rich in freshwater molluscs, mostly preserved as aragonite shells. The study focuses on 1) the sedimentological, paleontological and geochemical ($\delta^{13}C$ and $\delta^{18}O$) characterization of the carbonate deposits, to decipher the depositional, climatic, hydrological and ecological conditions of the lake systems, and their evolution through time, 2) the distinct sequential arrangement of facies and the proposal of a sedimentary facies model, 3) discerning conditions for calcareous biota development and their preservation, and 4) the influence of climate at different time scales and regional tectonism. The findings add to the knowledge of carbonate lake basins, help discern the factors that controlled their evolution and highlight specific depositional and preservation conditions for gastropod-rich carbonate records.

2. Geological setting

The Pyrenean range is a west-northwest to east-southeast oriented mountain belt developed during the Cenozoic by the collision of the Iberian and Eurasian plates, following the progressive tectonic inversion and uplift of the series of rift troughs and basins created along the Europe-north Iberia plate boundary during the Late Jurassic-Early Cretaceous opening of the Bay of Biscay (Muñoz, 2002, 2019; Teixell et al., 2016, 2018). Compressional tectonism began at Campanian times and progressed during the Paleogene and Neogene, with phases of stronger deformation during the middle-late Eocene, Eocene to Oligocene transition and Early-Middle Miocene times. The correlation of the syntectonic sedimentary record reveals that all Pyrenean basins already lost connection to the ocean and became fully continental by the latest Eocene (Hogan and Burbank, 1996; Costa et al., 2010; Garcés et al., 2020; Larena et al., 2024). The subsequent Oligocene to Miocene depositional history was a combination of tectonic shortening, continued uplift and denudation, and the deposition of thick alluvial and lacustrine successions along the northern (Aquitaine) and southern (Ebro) flanking forelands and, to a minor extent, on small intramontane basins associated to the northern and southern Pyrenean thrust belts (Plaziat, 1981; Muñoz, 2002; Costa et al., 2010; Ortiz et al., 2020; Garcés et al., 2020; Larena et al., 2024).

The study area is located in the Miranda-Trebiño basin, on the southern Basque-Cantabrian Pyrenees or western Pyrenean domain. This is a piggy-back basin developed over a series of south-verging folds and thrust sheets, at depth rooted on a basal detachment thrust plane that emerges at surface along the Montes Obarenes and Sierra de Cantabria ranges. This structure represents the western prolongation of the south Pyrenean Thrust Front (SPTF in Fig. 1A) and marks the boundary between the hinterland and the youngest southern foreland basin (i.e., the Ebro Basin). The Miranda-Trebiño Basin extends for about 30–40 km east-west and 10–15 km north-south. The basin infill consists of 1500–2000 m of syntectonic Palaeogene to Neogene succession comprising proximal alluvial deposits grading to lacustrine carbonates, the latter best developed across the central and southern basin domains. The succession is arranged in three main unconformity-bounded megasequences overlapping the folded and tilted substrate consisting of Cretaceous-lower Palaeogene marine sequences (Riba, 1956, 1961; Martín-Alafont et al., 1978; Larena et al., 2024). The development and extent of these syntectonic megasequences was largely controlled by the raise of the SPTF, a progressive northwards basin tilting and depocentre migration and, at local scale, by the raise of Triassic-cored diapirs and salt walls (i.e. Salinas de Añana, Trebiño and Peñacerrada diapirs).

The Peña Adrian Formation (PAF on Fig. 1A) is the youngest depositional unit of the Miranda-Trebiño Basin. It is exposed in two main hill outcrops on the southern margin of the basin and, according to the initial definition of Riba (1956, 1961), largely represents a post-tectonic depositional unit over the thick northward-tilted Oligocene megasequence and the Cretaceous-Paleocene marine substrate (Fig. 1B). The formation reaches a maximum thickness of 160 m and comprises two main lithological ensembles: alluvial deposits and lacustrine-palustrine carbonates containing abundant mollusc fossil biotas. The upper boundary, only well exposed at the Cantera section (Fig. 1B), is also an erosional discontinuity separating the topmost lacustrine carbonates from coarse alluvial deposits attributed to the Pliocene (Portero García et al., 1976). Based on the general stratigraphic context, the unit was formerly attributed to the Late Miocene-Pliocene (Portero García et al., 1976). The recent analysis of charophyte and ostracod associations (Larena et al., 2023), however, has allowed constraining the formation to the Tortonian (Late Miocene).

3. Database and methods

The analysis of the Peña Adrian Formation is a field-based study implying the mapping, logging and correlation of six stratigraphic sections measured at 1:100 scale (Figs. 1B, 2). From northwest to southeast, these sections are: Morro (MO), Falla (FA), Depósito (DE), Valverde (VA), Cantera (CA) and San Miguel (SM) (Fig. 1B). The resulting correlation scheme (Fig. 2A) was constructed through lateral tracing of several key beds and bed intervals and the interpretation of photomosaics and aerial photographs.

A total of one hundred and ten oriented rock samples of detrital (i.e., formed of extrabasinal sediment) and carbonate composition were collected to study the microfacies, mineralogy and C—O stable isotopes (Tables S1, S2). Seventy thin sections were performed at the Rock Processing Lab (SGIKER) of the University of the Basque Country (UPV-EHU), Spain for the petrographic analysis, textures, microfossil

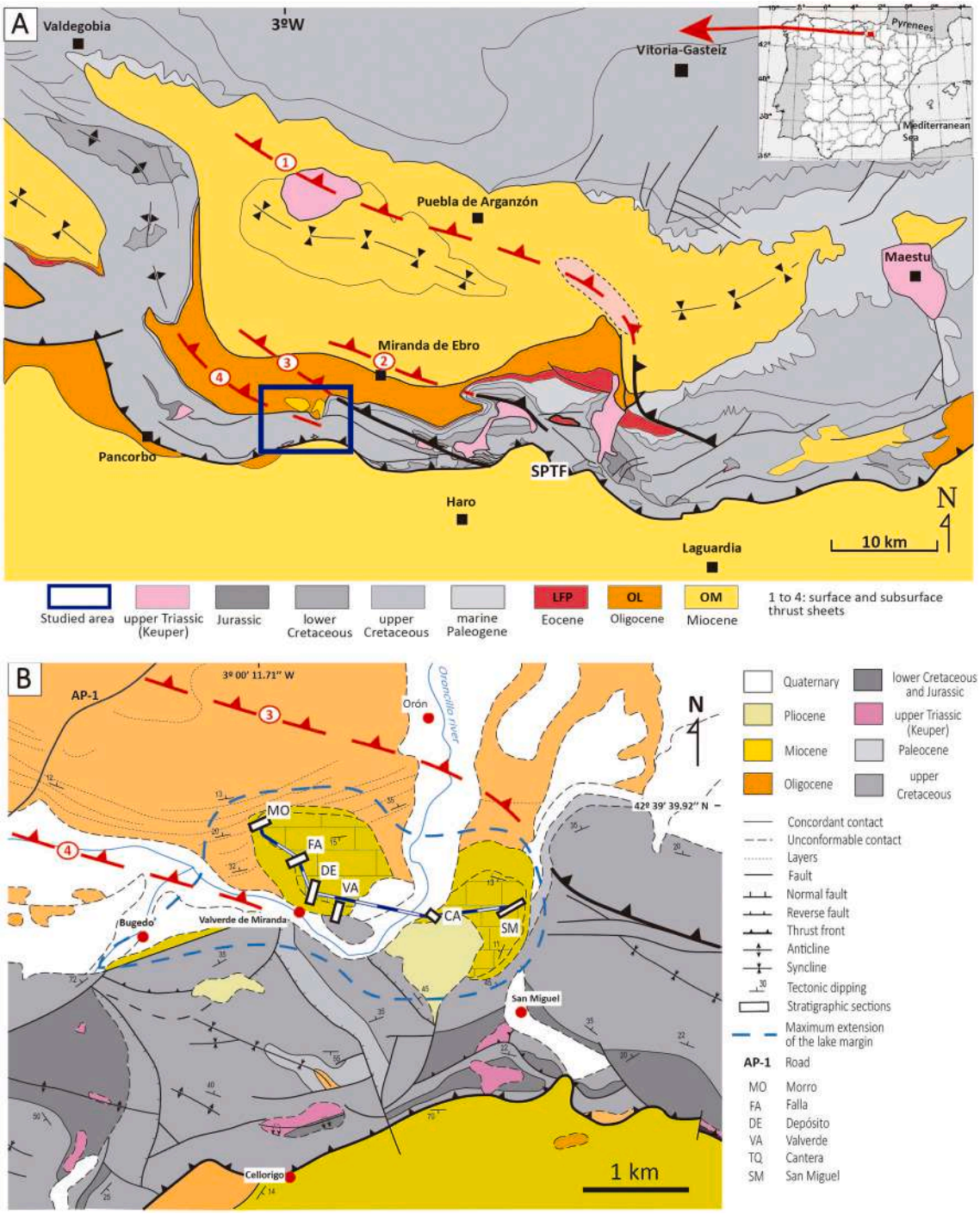

Fig. 1. A) Geological map of the Miranda-Trebiño Basin, in the blue box the studied area. 1 to 4 indicate the surfaces and subsurface thrust sheets. B) Geological map of the study area with the location of the six detailed sections of the Peña Adrian Formation. The blue line represents the proposed maximum extension of the lake margin.

abundance and diagenetic attributes, using a petrographic microscope equipped with digital camera and software for image capturing. Fifteen samples were studied by scanning electron microscopy using a Carl Zeiss MERLINTM FESEM, Zeiss AG, operating at 3-15 kV and 158 pA in the research facilities (*Servicios de Apoyo a la Investigación*, SAI) of the University of Zaragoza (UZ), Spain. The classification of the carbonate samples was based on Dunham (1962), Embry and Klovan (1971), Flügel (2004) and Alonso-Zarza and Wright (2010).

3.1. Mineralogy and stable isotope analysis

The mineralogical composition of fifty-three carbonate rock samples and three samples of gastropod shells was determined by X-ray diffraction (XRD) at the X-Ray Laboratory (SGIKER) of the UPV-EHU using a PANalytical CubiX diffractometer, equipped with copper tube, vertical goniometer, programmable slits, automatic sample exchanger, filter nickel and PixCel detector. The measurement conditions have been 40 kV and 40 mA, with a sweep between 5 and 70° 2 theta's from some samples. Powders for mineralogical and isotopic analysis were extracted

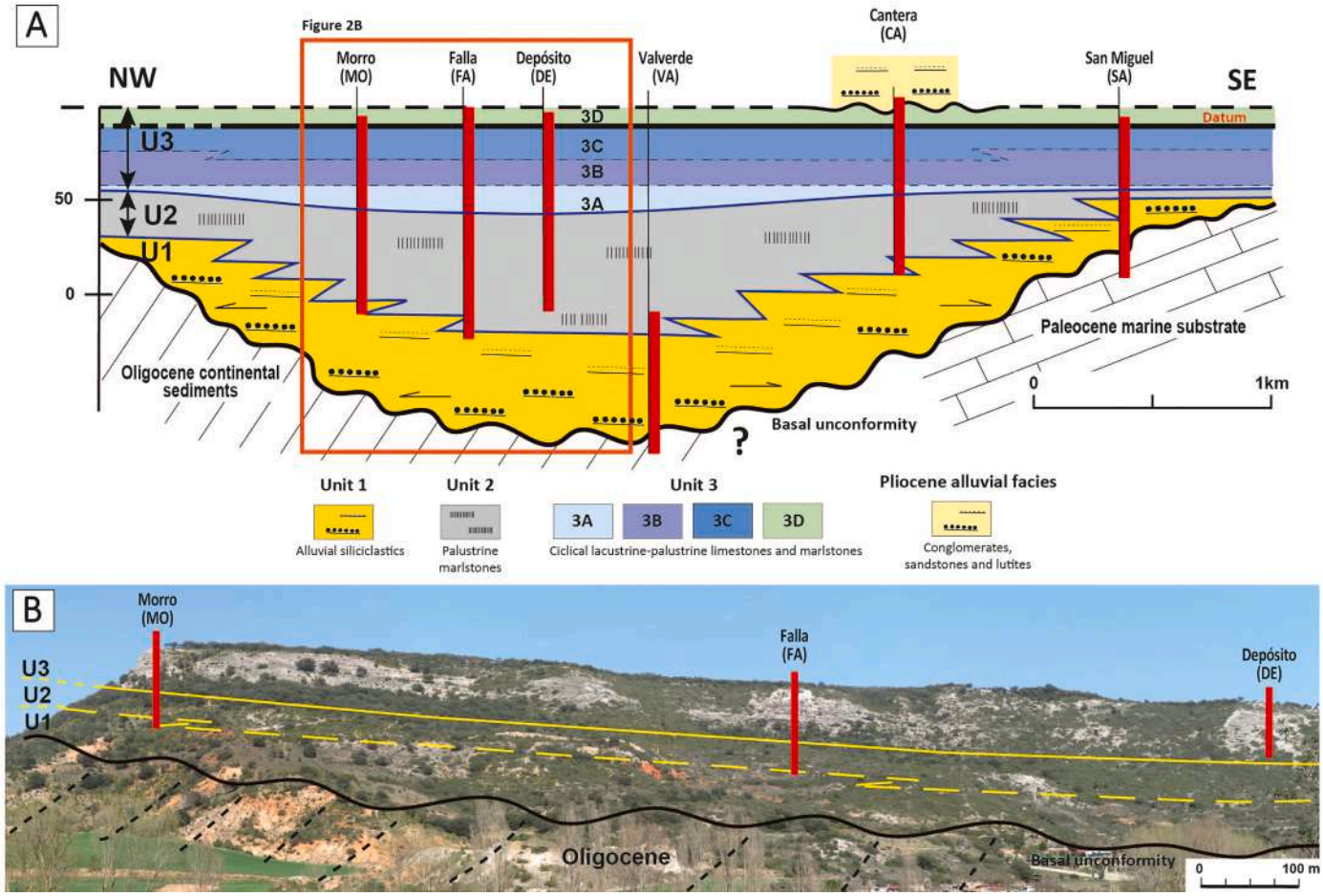

Fig. 2. A) General stratigraphic and facies architecture of the Peña Adrian Formation, Datum of the correlation of the six sections located at the top of Unit 3 described by the net change of carbonate facies. Internal facies architecture of the three units: Unit 1 (alluvial deposits), Unit 2 (palustrine carbonates) and Unit 3 (palustrine-lacustrine carbonates). Basal angular unconformity with the Oligocene and Paleocene substrate. B) Outcrop photograph of the northwestern sections. Note the unconformable relation between the described units and the Oligocene substrate.

using a microdrill, from the most pristine areas of the samples (mainly matrix sediment) lacking diagenetic overprint (i.e. neomorphism and cement phases).

The $\delta^{13}C$ and $\delta^{18}O$ analyses of fifty nine samples have been performed in the *Centres Científics i Tecnològics* of the University of Barcelona (UB), Spain. The ratios were measured in a mass spectrometer (MAT-252, Thermo Finnigan; Thermo Fisher Scientific, Waltham, MA, USA), following standard procedures for calcite (McCrea, 1950). The international standards NBS-18 ($\delta^{13}C$ = -5.1 ‰ VPDB; $\delta^{18}O$ = -23.01 ‰ VPDB) and IAEA-603 ($\delta^{13}C$ = 2.46 ‰; $\delta^{18}O$ = − 2.37 ‰ VPDB), and internal RC-1 ($\delta^{13}C$ = 2.78 ‰ VPDB; $\delta^{18}O$ = -2.08 ‰ VPDB) were used to calibrate $\delta^{13}C$ and $\delta^{18}O$ to the Vienna Pee-Dee Belemnite (VPDB). The overall reproducibility was better than 0.02 ‰ and 0.04 ‰ for $\delta^{13}C$ and $\delta^{18}O$ respectively. Results are reported in δ ‰ notation relative to VPDB (Table S2).

Dolomite and aragonite were not removed from carbonate and marl samples prior to isotopic analyses due to the difficulties with this procedure (Sreenivasan et al., 2023; Yui and Gong, 2003). Carbonate samples containing those minerals were analysed following calcite protocols. A correction factor proportionate to the dolomite or aragonite content respect to the total carbonate content has been applied to $\delta^{13}C$ and/or $\delta^{18}O$ values of samples containing those minerals (as explained below). The corrected values are used as an estimation of the isotopic values of calcite, to be comparable with other calcite values (Table S2).

There is no consensus about the ^{18}O enrichment of dolomite $\delta^{18}O$ with respect to calcite in natural environments (Murray and Swart, 2017 and references therein). In this work, dolomite $\delta^{18}O$ enrichment with respect to calcite has been corrected by 4 ‰ proportionate to dolomite vs total carbonate content in each sample, as described by Arenas et al. (1997, 2024). As discussed below (Section 5.2.2), dolomite is considered a primary precipitate that formed from the same water parents as calcite (cf. Arenas et al., 2024). The correction provides an estimation of the $\delta^{18}O$ values of calcite that would have coexisted with dolomite. Only one sample contains significant dolomite percentage. No correction has been applied to $\delta^{13}C$ values, as the relationship between $\delta^{13}C$ and dolomite content is unclear, and the dolomite $\delta^{13}C$ enrichment is much smaller than that of $\delta^{18}O$ (Arenas et al., 1997, 2024; Horita, 2014; Valero-Garcés et al., 2000).

The abundance of gastropod whole shells and fragments in most samples suggests that the aragonite content in the extracted powder is of bioclastic origin. Different fractionation mechanisms, including variability of vital effects affecting primarily $\delta^{13}C$, are involved in ^{13}C and ^{18}O enrichment of aragonite with respect to calcite. The approximate $\delta^{13}C$ and $\delta^{18}O$ values corresponding to calcite can be estimated by using correction factors. Three samples containing significant amounts of aragonite (> 30 % of total carbonate) have been excluded from calculations and evolutionary trends to avoid uncertainties. The isotopic values of samples containing up to 21 % of aragonite vs total carbonate content have been corrected as follows (Table S2). The calcite $\delta^{18}O$ values have been calculated by using the difference of ca 0.8 ‰ aragonite-calcite fractionation at 25 °C, obtained by Kim et al. (2007) for equilibrium conditions. For the calcite $\delta^{13}C$ values, the difference of

aragonite-calcite fractionation of 1.7 ± 0.4 ‰ at temperatures between 10 and 40 °C estimated by Romanek et al. (1992) has been used.

The $\delta^{13}C$ and $\delta^{18}O$ values were smoothed through LOESS (Locally Estimated Scatterplot Smoothing) of the statistical program PAST software (Hammer et al., 2001; https://www.nhm.uio.no/english/research/resources/past/).

3.2. Paleontological analysis

The Peña Adrian lacustrine deposits are rich in fossil calcareous biotas, including gastropods, ostracods and charophyte. Eight samples from poorly-indurated sediments were collected for taxonomic determinations: two from limestone-marlstone beds of Unit 2 and six from layered limestone-marlstone intervals within subunits 3A to 3C (sample location in Fig. 3). Three kilogram of sediment per collected sample were washed and sieved using 2-, 0.5- and 0.16-mm mesh light sizes.

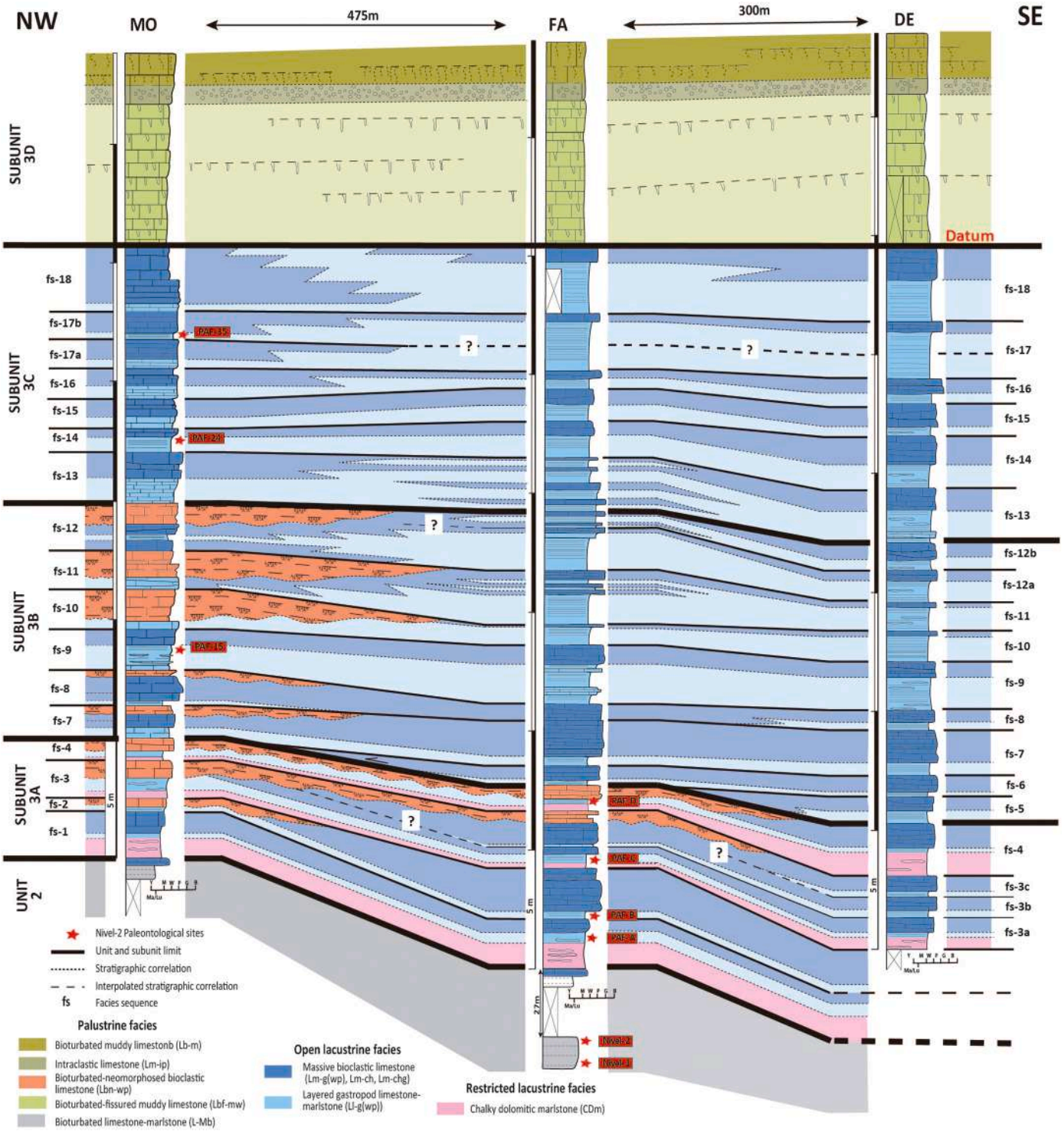

Fig. 3. Detailed correlation of the northwestern stratigraphic sections, location in Figs. 1B and 2A. The datum is the net change of lacustrine facies of subunit 3C to palustrine facies of subunit 3D. Identified facies sequences (fs) are represented and numbered.

Table 1
Paleontological content (presence of ostracods, charophytes and gastropods) of the ten samples collected in units 2 and 3.

	Unit 2		Unit 3							
	Nivel 1	Nivel 2	Subunit 3A				Subunit 3B	Subunit 3C		
			PAF-A	PAF-B	PAF-C	PAF-D	PAF-15	PAF-24A	PAF-24B	PAF-35
Ostracods										
Candona sp.							X	X		
Cypridopsis vidua (O. F. Müller, 1776)					X	X				
Cypris bispinosa (Lucas, 1849)	X	X	X	X	X	X	X	X	X	
Darwinula stevensoni (Brady y Robertson, 1870)							X	X	X	X
Ilyocypris bradyi (Sars, 1890)			X	X	X	X		X	X	X
Ilyocypris gibba (Ramdohr, 1808)			X			X		X		
Paralimnocythere psammophila (Flösner, 1965)							X			
Pseudocandona eremita (Vejdovsky, 1882)	X				X	X				
Pseudocandona marchica (Hartwig, 1899)						X				
Pseudocandona parallela (G.W. Müller, 1900)			X	X		X	X	X	X	X
Charophytes										
? *Lychnothamnus* sp.	X	X								
Chara sp.	X									
Chara cf. *molassica* var. *notata* (Straub, 1952; Soulié-Märsche, 1989)			X	X		X	X	X	X	
Gastropods										
Gyraulus laevis							X	X	X	
Mercuria sp.		X	X	X	X	X	X	X	X	X
Bithynia sp.			X	X			X	X	X	
Stagnicola sp.		X		X	X	X	X	X	X	X
Ancylus sp.		X								
Segmentina sp.	X	X		X						
Planorbis sp. 2	X				X					
Planorbis sp. 1						X				

The sediment fractions >2 and >0.5 mm were studied for gastropod determinations, and those between 0.16 and 0.5 mm for charophyte and ostracods. A SEM Quanta 200 equipment (CCiTUB, Barcelona) was used for imaging of charophytes and a stereomicroscope (Nikon SMZ-U, Bilbao) for ostracods and gastropods. Table 1 summarised the results of the paleontological study, including previous paleontological data from two samples collected in the same area (Larena et al., 2023). The semi-quantitative analysis of thirty-two thin sections, rock slabs and several clean outcrops provided additional information about the relative abundance and distribution of the fossil biotas in the indurated deposits of subunits 3A to 3D. Small (<3 mm) gastropods dominate in most bioclastic beds, along with smaller quantities of medium-large (3–30 mm) gastropods, ostracods and charophyte. The relative abundance of small gastropods, expressed in number of specimens per square centimetre, was established through specimen counting from 4 cm^2 areas in thin sections and from 25 cm^2 quadrats in polished rock slabs and clean surfaces of selected beds at outcrop. Aside from marked variation in relative abundance depending on facies types, the calcareous biota exhibits different degree of preservation in terms of mineralogy and microstructure, due to contrasting early diagenetic modifications (see below). Among gastropods, the most abundant bioclastic component, good, poor and bad preservation categories can be distinguished. Good preservation refers to shells keeping their primary single aragonitic or bimineralic, (calcite+aragonite) layers of lamellar to homogenous microstructure. Poor preservation, instead, refers to shells affected by moderate to intense neomorphism to calcite, and partial to complete loos of original microstructure. Finally, bad preservation mainly results from partial to complete dissolution of the shells, producing moulds and steinkers in the sense of Wright et al. (2018), with or without late calcite cement fills. Charophyte remains (calcified parts of gyrogonites and stems) usually exhibit poor to bad preservation due to low primary calcification, neomorphism, encrustation and cement overgrowths or combination among these processes. In contrast, ostracod caparaces commonly exhibit good preservation and, in several washed residues, shells of pristine calcite are relatively common.

4. Results

4.1. Stratigraphic arrangement

The correlation of the six stratigraphic sections logged across the study area provided the large-scale stratigraphic architecture of the Peña Adrian Formation, which ranges in thickness between 50 and 160 m (Fig. 2A). Three lithological units, arranged in gradual vertical and lateral transition, are distinguished: a basal detrital (consisting of extrabasinal sediment) Unit 1 (U1), a middle unit of mixed carbonate-fine detrital (consisting of extrabasinal sediment) nature Unit 2 (U2) and an upper carbonate-dominated Unit 3 (U3).

Unit 1 comprises the basal 8–50 m and consists of fine to coarse alluvial detrital deposits. The dominant facies are reddish massive to laminated sandy mudstones with prominent colour mottling and sparse root traces (facies Lut, Table S1). They occur interbedded with metre-thick beds of massive, poorly sorted conglomerates and pebbly sandstones (facies Ss and Cgl, Table S1) consisting of a high proportion of lithoclasts (bioclastic limestones, dolostones and sandstones), from different units of the Cretaceous to Paleocene marine basin substrate.

Unit 2, with a maximum thickness of 60 m, is mostly made of massive to laminated grey limestone-marlstones (facies L-Mb, Table S1), containing moderate-abundant silt-sized quartz grains and sparse remains of gastropods, ostracods and charophyte. The limestone-marlstones beds include thin interbeds of reddish lutites and comprise discontinuous horizons of rhizogenic calcretes (facies Calc, Table S1). The unconsolidated nature of this facies ensemble only provides outcrops of moderate-bad quality and sparse occurrence, a situation that prevents continuous logging and a detailed observation of bedding features and facies arrangement.

Unit 3, 34 to 40 m thick, mostly consists of indurated carbonate deposits forming stepped cliffs, representative of different palustrine and lacustrine depositional settings (see below). The study focused through the 775-m long outcrop between Morro (MO) and Depósito (DE) sections (Fig. 2B), complemented with information from the Cantera and San Miguel sections. According to changes in their constituent facies and vertical sequential arrangement, Unit 3 can be subdivided into four subunits (3A to 3D in Figs. 2A, 3), each ranging from 8 to 13 m in thickness.

As for the stratigraphic relationships between these units, U1 and U2 are laterally related, with a clear expansive character of Unit 2 over the basin margins. The boundaries between Units 2 and 3, and between subunits 3A to 3D correspond to sharp facies changes that locally also exhibit erosion and features of subaerial exposure. Detailed stratigraphic correlation reveals that the boundary between subunits 3A and 3B also corresponds to an onlap towards the Morro section (Fig. 3).

4.2. Facies analysis and facies associations

Up to thirteen individual sedimentary facies have been distinguished

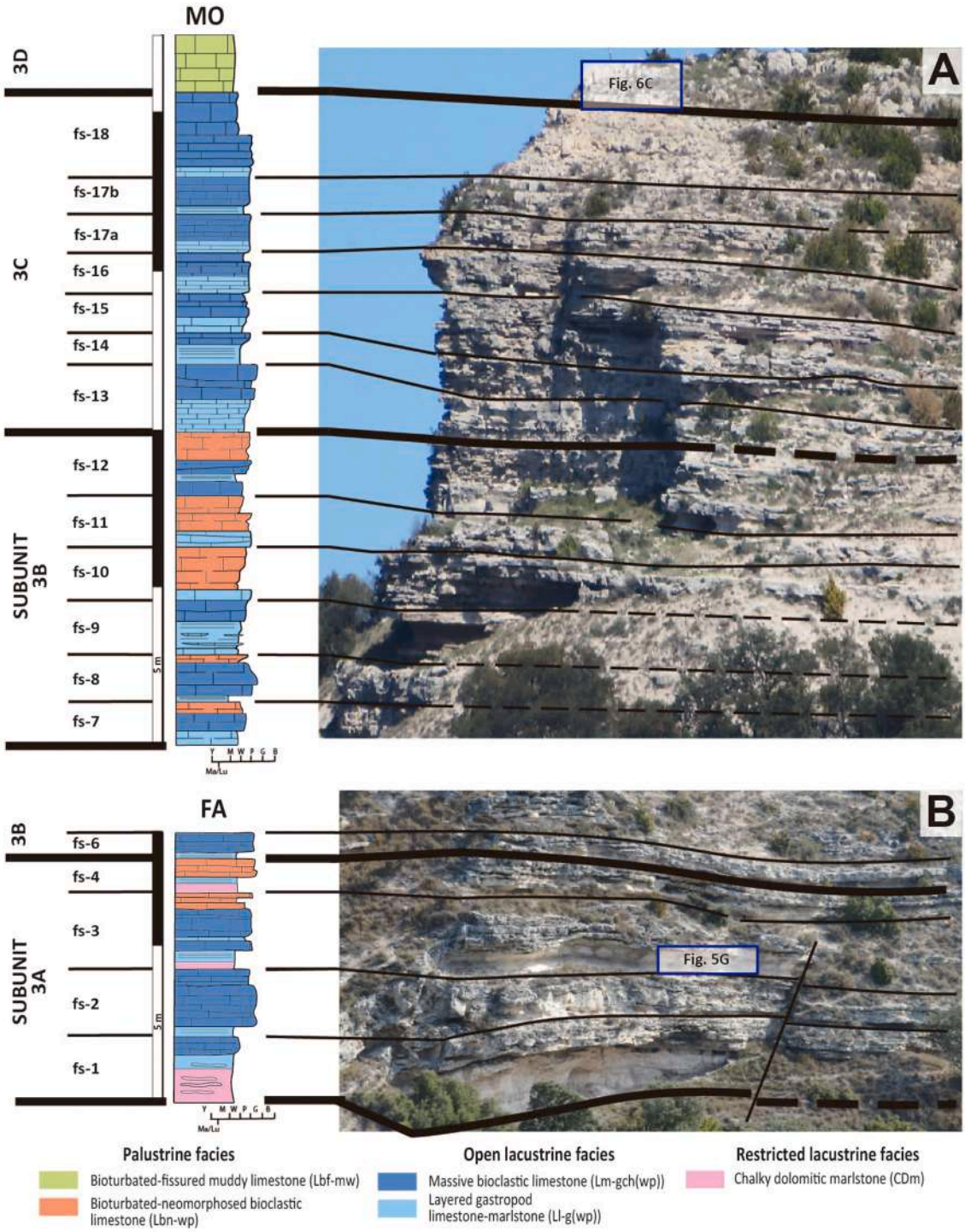

Fig. 4. Outcrop photographs and their corresponding stratigraphic sections (Morro section (MO) and Falla section (FA)), location in Fig. 3. Note the vertical distribution of the facies and the inferred facies cyclicity. See location in Fig. 3.

in the Peña Adrian Formation according to their lithology, textural characteristics, bedding style, sedimentary structures, diagenetic features and biotic content. Table S1 summarizes their key features and interpretation in terms of sedimentary processes and prevailing conditions during deposition. The succession comprises alluvial, extrabasinal sediment-made deposits, and a variety of carbonate facies, mainly limestones with variable content of aragonite and dolomite. The facies analysis focuses on the carbonate and mixed deposits that form the bulk of Units 2 and 3 of the Peña Adrian Formation The detailed correlation scheme in Fig. 3 shows the complex spatial distribution and interrelationships of all deposit types across the outcrop segment between the Morro and Depósito sections (location in Fig. 2B), while Fig. 4

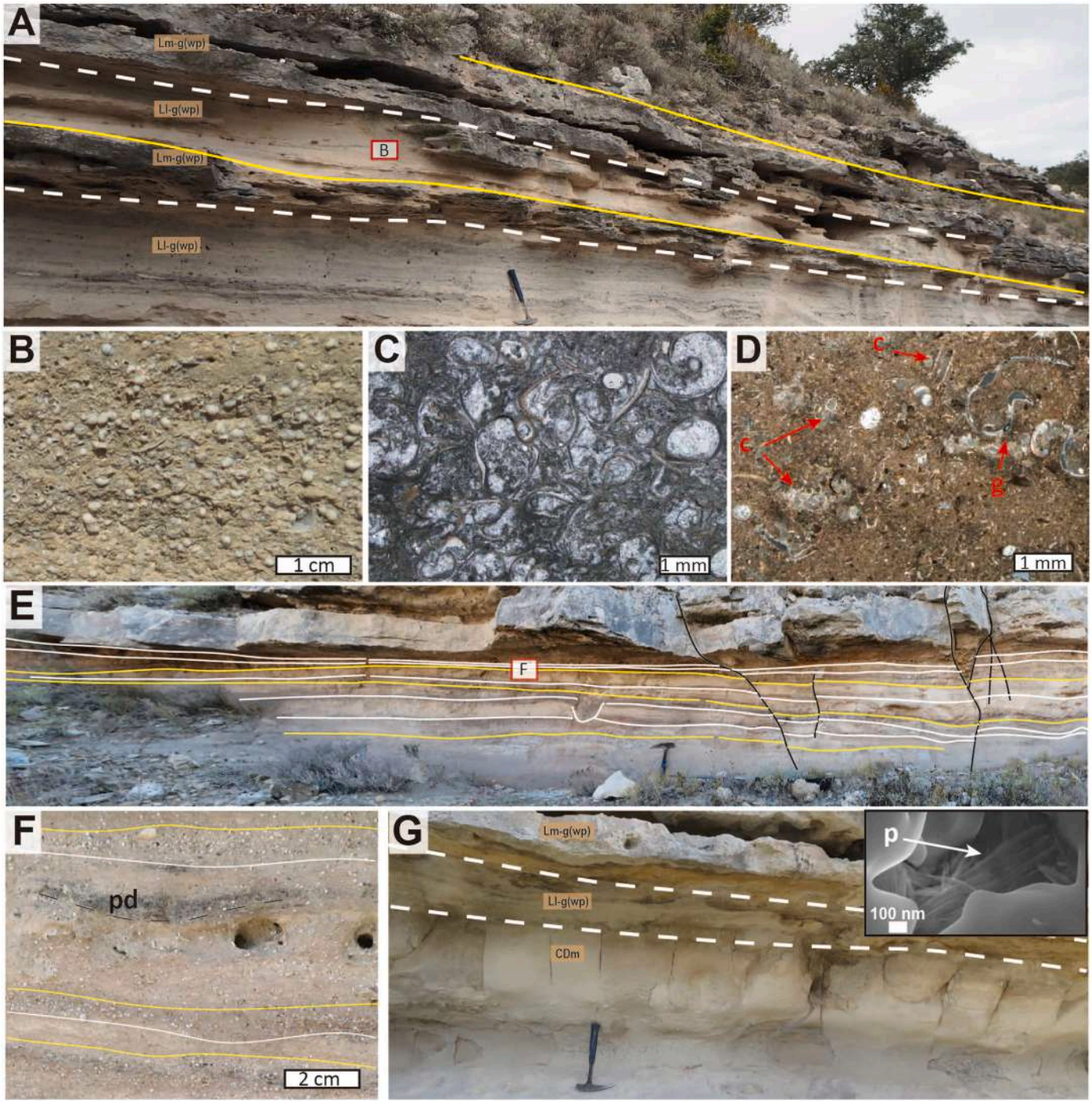

Fig. 5. Outcrop photographs and microfacies of open and restricted lacustrine facies (FA2 and FA4). A) Two stacked facies sequences consisting of layered gastropod limestone-marlstone (Ll-g(wp)) and gastropod limestone (Lm-g(wp)). B) Close up of gastropod limestone note the large number of gastropod individuals. C) Microphotograph of gastropod "coquina" of the facies gastropod limestone note the good preservation of gastropods aragonite shells. D) Charophyte-gastropod wackestone-packstone (Lm-chg) with high number of charophyte thally and gyrogonites and gastropod fragments. E) Layered gastropod limestone-marlstone where the lateral continuity of the different layers can be observed. Note the irregular shape and sedimentary compensation of some layers. F) Close up of layered gastropod limestone-marlstone, consisting of some layers with high proportion of gastropod individuals and others with lees proportion. Intercalated marlstone layers with coalified plant debris (pd). G) Typical facies sequence of subunit 3A (Figs. 3, 4) with whitish massive chalky dolomitic marlstone (CDm) of the restricted lacustrine facies association (FA4) at the base. Note the SEM image of palygorskite from the massive chalky dolomitic marlstones.

presents the vertical distribution of facies at the base of the Falla section and the Morro section. Figs. 5 and 6 illustrate representative examples of facies at outcrop scale and microfacies.

4.2.1. Detrital facies

These consist of lutites, sandstones and conglomerates (facies Lut, Ss and Cg) formed of extrabasinal calcareous and siliceous sediment from the basin bounding units. They form the bulk of Unit 1 (Fig. 2A) and represent extensive distal alluvial mud flats that received channelled and unconfined water flows with coarse to fine sediment.

4.2.2. Massive bioclastic limestones

The deposits of this group are the most abundant within the subunits 3A to 3C. They form massive tabular strata, 13 to 55 cm thick (Fig. 5A to D). Gastropods and charophyte gyrogonites, along with minor amounts of charophyte stems and ostracods, are the main allochems in these facies. According to texture and relative proportion of gastropods and charophytes, three main facies types in gradual vertical and/or lateral transition can be distinguished: gastropod wackestone-packstones (Lm-g (wp)), charophyte mudstone-wackestone (Lm-ch) and, transitional between them, charophyte-gastropod wackestone-packstones (Lm-chg) (Table S1). The three varieties comprise small (<3 mm) planispiral and

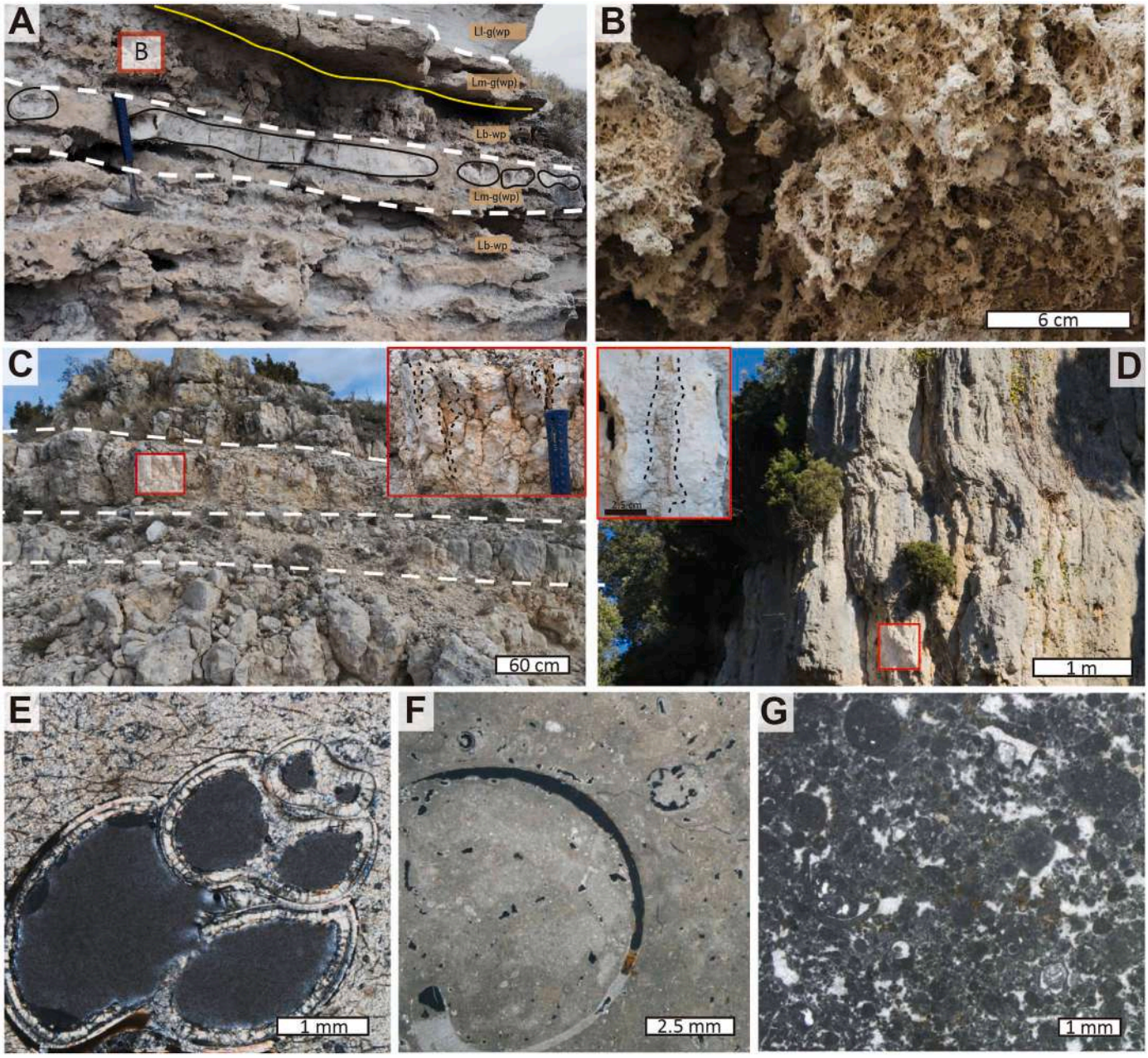

Fig. 6. Outcrop photographs and microfacies of palustrine facies (FA3). A) Two stacked facies sequences of bioturbated-neomorphosed bioclastic limestone (Lbn-wp) (FA2) and gastropod limestone (Lm-g(wp)) (FA3). Note the interval with silex nodules in the bioturbated-neomorphosed bioclastic limestone strata. B) Close up of bioturbated-neomorphosed bioclastic limestones with root traces of different sizes. C) Bioturbated-fissured muddy limestones (Lbf-mw) with abundant areas having fissures, cracks and brecciation. Note the root traces with reddish fillings. D) Bioturbated muddy limestones (Lb-m). Note the presence of vertical to subvertical fissures and occasional root marks. E) Microphotograph of silicified gastropod shell in elongated silex nodule, location of the nodule in Fig. 4A. F) Bioturbated muddy limestone (Lb-m), note the partial and/or total dissolution of the bioclasts. G) Close up of intraclastic limestone (Lm-ip) including micrite intraclasts and in less proportion bioclasts.

trochospiral gastropods of aragonitic or bimineralic compositions with good shell preservation (Fig. 5B to D), plus lesser amounts of larger gastropods (3–30 mm) showing different degree of flattening and fragmentation by compaction. The matrix in all of them consists of micrite with variable amounts of peloids, tiny bioclastic fragments, sparse coalified plant remains and disseminations of iron sulphides.

The diagenetic imprint in these massive bioclastic limestones mainly consists of compactional features evidenced by gastropod shell flattening and in situ breakage (Fig. 5C). Neomorphism affects locally the micrite and microbioclastic matrix, in some cases associated to compactional sub-mm dissolution seams.

4.2.3. Layered carbonate facies

This is the second most abundant facies type within subunits 3A to 3C. They consist of cm-thick wackestones and packstones with small planispiral and trochospiral gastropods, alternating with mm-thick, discontinuous marlstone interbeds (Fig. 5E). Locally, mollusc shells form thin discontinuous coquina layers (Fig. 5F). In the outcrop, this characteristic facies occurs forming m-thick recessive intervals that can be traced laterally across 100's of meters. Most marlstone interbeds consist of a mixture of clays, silt-sized quartz grains, comminute coalified plant debris and reworked gastropod shells and fragments. Ostracods are common and charophyte gyrogonites occur locally in both terms.

Differential carbonate cementation is common and evident at outcrop, in the form of bed-parallel calcite nodules engulfing both limestone and marlstone interbeds. Sparry and blocky calcite cements fill matrix voids and gastropod intra-shell voids, commonly overlaying muddy-peloidal geopetal sediment.

4.2.4. Bioturbated carbonate facies

This group includes deposits with evidence of root traces, breakage, desiccation, oxidation and/or reworking. Up to five distinct facies types can be distinguished: bioturbated limestone-marlstone (L-Mb), rhizogenic calcrete (Calc), bioturbated-neomorphosed bioclastic limestone (Lbn-wp), bioturbated-fissured muddy limestone (Lbf-mw), intraclastic limestone (Lm-ip) and bioturbated muddy limestone (Lb-m) (Table S1).

The bioturbated limestone-marlstones (L-Mb) are the bulk facies of Unit 2, but also occur as discrete interbeds in Unit 3. Within Unit 2, they form extensive and poorly-consolidated intervals ranging 0.5 to 5 m in thickness, of dominant grey colour and with discontinuous lamination. They comprise abundant small gastropods, ostracods and charophyte gyrogonites, all with disperse distribution. Sub-vertical root traces are common in most outcrops, locally forming layers of immature rhizogenic calcretes (Calc). These are whitish indurated carbonate horizons, 30–60 cm in thickness, that are mainly identified by calcified subvertical root marks combined with moderate brecciation-fissuring and red-yellowish irregularly shaped oxidized zones.

The bioturbated-neomorphosed bioclastic limestones (Lbn-wp) are distinct facies in subunits 3 A and 3B, particularly in the Morro section, where they form up to eight characteristic bed intervals ranging 0.2–2 m in thickness (Figs. 3, 4). They consist of bioclastic wackestones and packstones with differential dissolution and neomorphism affecting both the matrix and allochems. At outcrop, the most distinct feature of this facies is the development of mesh works of cm-long subvertical rhizoliths (Fig. 6B), commonly coated with gastropod fragments. Discontinuous levels of ellipsoidal to elongated secondary chert nodules, up to 0.5 m long (Fig. 6A), occur intimately associated with facies Lbn-wp commonly engulfing both bioclasts and micrite matrix (Fig. 6E).

The bioturbated-fissured muddy limestones (Lbf-mw) are bioclastic mudstones and wackestones forming a characteristic interval at the base of subunit 3D, laterally continuous between the Morro and Depósito section (Fig. 3), and across the outcrops between Cantera and San Miguel (Fig. 2A). They form tabular indurated strata, up to 2 m thick, with irregular and discontinuous bases and tops (Fig. 6C). A dense and homogenous micrite matrix containing very sparse gastropods, ostracods and charophyte stems and gyrogonites, plus a minor fraction (1–2 %) of silt-sized subangular quartz grains, characterizes this facies. Disseminations of iron sulphides (pyrite?) are evident in thin section. The very sparse fossil remains are mainly preserved as empty moulds (Fig. 6F) and steinkerns, in the sense of Wright et al. (2018). Local brecciation and staining by iron oxides, both as patches and disseminations, commonly occur associated with subvertical to irregular root traces and dissolution fissures.

The intraclastic limestones (Lm-ip), also characteristic of subunit 3D, form a 1–2 m thick interval overlying the basal Lbf-mw facies and are also recognized as thin discontinuous interbeds within strata with facies Lb-m. They form brechoid to massive strata of dominant wackestone-packstone texture with abundant peloids and subrounded micrite intraclasts concentrated in the brecciated zones. Their fossil content comprises charophyte stem and gyrogonites (commonly neomorphosed) and gastropods moulds partially filled with sparry calcite.

The bioturbated muddy limestones (Lb-m) define the topmost bed interval of subunit 3D across the whole the study area. They occur arranged in m-thick, laterally-continuous massive beds composed of dense and homogeneous dark grey micrite with a minor bioclastic fraction of recrystallized or dissolved charophyte gyrogonites and stems, and very sparse gastropod moulds. At outcrop, the most distinct features are decimetre-long subvertical irregular root traces and fissures lined by iron oxides and locally filled with intraclastic, brechoid sediment (Fig. 6D). These structures form networks that deepen 0.5–2 m, cutting across primary bedding surfaces and, attending to the variety of filling material, seem to have recorded a polyphasic development.

The dissolution and/or moderate-intense neomorphism affecting the bioclastic fraction and matrix are common in all of the bioturbated carbonate facies. The most distinct neomorphic features occur in the facies Lbn-wp intervals, disrupting the regular stratification in combination with heterogeneous cementation. Sparry and drusy calcites are common cement phases filling all primary and secondary voids associated to cracking and fissuring, as well as in channel and breccia fabrics (Fig. 6C, D).

4.2.5. Dolomitic marlstone

These deposits are minor and exclusive to subunit 3A and comprise a single facies type: cream to whitish, chalky dolomitic marlstones (CDm). They form structureless poorly-indurated intervals, 0.3–2 m thick (Fig. 5G), which can be traced over hundreds of meters laterally (Fig. 3). These intervals are better developed and thicker in the central sections of the study area (i.e. Depósito section), and gradually loose entity and thickness towards the northwest (i.e. Morro section, Fig. 3). Microscopically, facies CDm consists of mosaics of very fine-grained subhedral to anhedral calcite and dolomite crystals, the latter representing up to 90 % in volume in some samples. Up to 20 % of palygorskite has been identified in a few samples (Fig. 5G; Table S2). Fossil components are lacking, with no evidence of having been removed by dissolution or replacement. Small traces of root marks and irregular desiccation cracks can be seen locally in all intervals.

4.2.6. Facies associations

The individual sedimentary facies described above (Table S1) can be grouped into facies associations (FA), based on integration of mineralogical composition, texture, sedimentary structures and biological attributes, which are representative of four main depositional environments: alluvial (FA1), open lacustrine (FA2), palustrine (FA3) and restricted lacustrine (FA4). Their detailed interpretation is discussed in Section 5.3.

The detrital facies (FA1) are indicative of middle-distal alluvial zones, with rare channels and extensive floodplains recording intermittent subaerial exposure (Miall, 1996; Paredes et al., 2007; Scott and Smith, 2015). The massive bioclastic limestones and the associated layered carbonate facies (FA2) indicate settings lacking subaerial exposure and plant bioturbation, i.e. shallow open lacustrine areas, with

varying contribution of fauna and flora, hydrodynamic processes and sediment transport and supply (Sturm and Matter, 1978; Glenn and Kelts, 1991; Platt and Wright, 1992; Sáez et al., 2007; Gierlowski-Kordesch, 2010). The bioturbated carbonate facies (FA3) are representative of palustrine zones (likely fringes) defined by dense plant colonization, and subject to episodic subaerial conditions (Freytet, 1973; Freytet and Plaziat, 1982; Alonso-Zarza et al., 1992; Freytet and Verrechia, 2002). Finally, the dolomitic marlstone facies (FA4) indicate shallow lacustrine areas with moderate to intense evaporative conditions, recording precipitation of Mg-rich carbonate and clay deposition (Calvo et al., 1995; Rodríguez-Aranda and Calvo, 1998; Warren, 2006).

4.3. Calcareous biota

The presence of a rich and abundant bioclastic content is one of the most distinct features of the lacustrine-palustrine facies of the Peña Adrian Formation. The most representative bioclastic components are small gastropods along with variable proportions of large gastropods, ostracods and charophyte (Table 1; Fig. 7). The relative abundance and degree of preservation of all these components vary significantly depending on the facies group.

4.3.1. Gastropods

The two representative facies of the open lacustrine environment within subunits 3A to 3C (the Ll-g(wp) and Lm-g(wp) facies) contain high amounts of well-preserved small (<3 mm) gastropods plus smaller quantities of medium-large (3–30 mm) taxa. A fabric of unsorted whole shells dispersed within the muddy-microbioclastic matrix is characteristic in both facies types. A relative abundance of 5–20 specimens/cm^2 of small gastropods is the rule in all thin sections of wackestone-packstone texture from facies Lm-g(wp) (i.e. Fig. 5F). This high abundance is laterally persistent, as noticed by visual inspection of distinctive beds and bed intervals of both Ll-g(wp) and Lm-g(wp) facies across 10's m distances (Fig. 5A, E). Additionally, thin and discontinuous gastropod coquina layers, made of whole shells and shell fragments occur interspersed in many beds of both massive layered open lacustrine carbonates. Taxonomic determinations revealed that *Mercuria* sp. (Fig. 7J) is the most abundant gastropod in the eight samples of Ll-g(wp) facies from subunits 3A to 3C, followed by variable amounts of *Bithynia* sp., *Gyraulus laevis* and *Stagnicola* sp. A similar association was determined in the two samples of palustrine limestone-marlstones (facies L-Mb) from Unit 2, which additionally contain small amounts of *Ancylus* sp., *Segmentina* sp. and *Planorbis* sp. The preservation of gastropod shells is good to excellent in all samples analysed from the open lacustrine deposits.

The relative abundance of gastropod shells falls to <5 specimen/cm^2 in the laterally-equivalent bioturbated palustrine deposits of subunits 3A to 3C, in parallel to a significant decrease in their degree of preservation. This is particularly evident in the facies Lbn-wp (bioturbated-neomorphosed bioclastic limestone), in which small and large gastropod shells commonly occur partially dissolved and/or affected by moderate-intense neomorphism. The abundance of gastropods is lower in the three characteristic muddy palustrine deposits that characterize subunit 3D

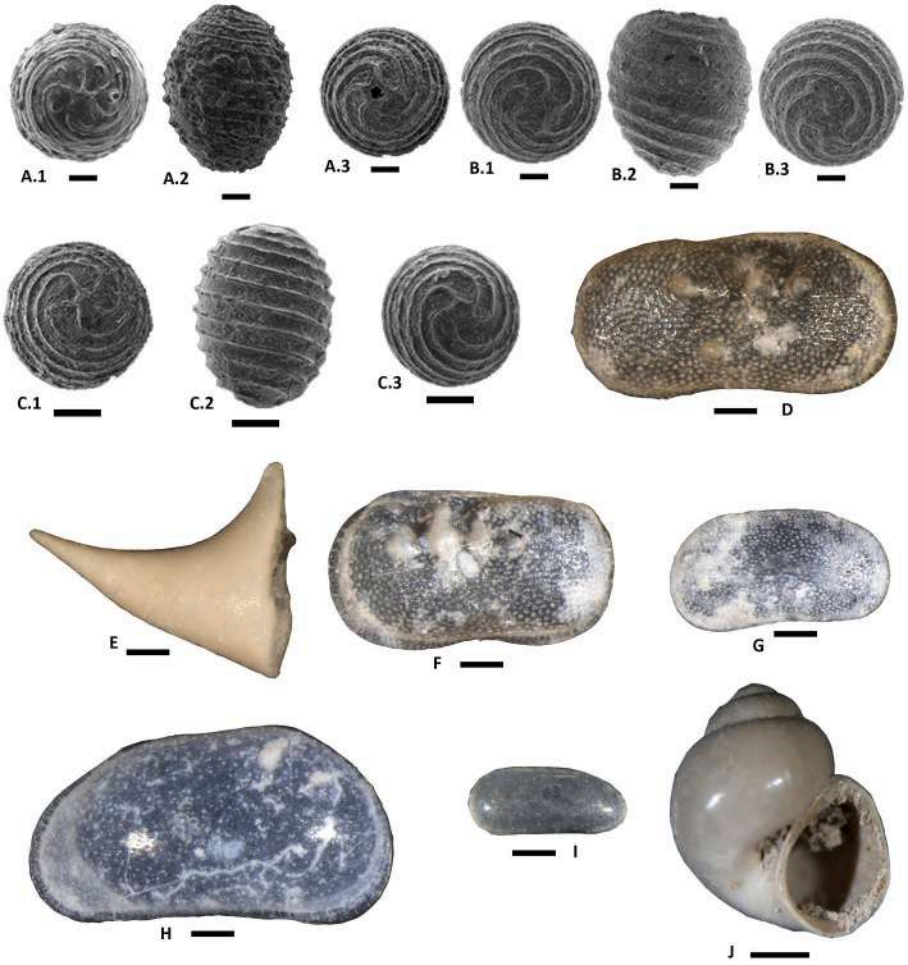

Fig. 7. Selected bioclast from carbonate facies. A) *Chara* cf. *molassica* var. *notata*. A.1. apical view, A.2. lateral view, A.3. basal view. B) ? *Lychnothamnus* sp. B.1. apical view, B.2. lateral view, B.3. basal view. C) *Chara* sp. C.1. apical view, C.2. lateral view, C.3. basal view. D) *Ilyocypris bradyi*. E) *Cypris bispinosa*. F) *Ilyocypris gibba*. G) *Pseudocandona parallela*. H) *Pseudocandona marchica*. I) *Darwinula stevensoni*. J) *Mercuria* sp. Scale bars for 1 to 8 = 0.1 mm. Scale bar for image 9 = 0.5 mm.

(the Lbf-mw, Lm-chg and Lm-ch facies), with sparse gastropod shells mostly preserved as empty moulds and steinkerns.

4.3.2. Ostracods

Ten different ostracod taxa were identified in the ten samples studied from Unit 2 and subunits 3A-C. They are comparatively abundant in the two levels of palustrine limestone-marlstones (L-Mb) from Unit 2, but with a monospecific association of *Cypris bispinosa* (Fig. 7E) plus scarcer *Pseudocandona eremita* (Table 1). Ostracods are more varied in the eight samples analysed from the open lacustrine facies of subunits 3A to 3C, with an association dominated by *Cypris bispinosa* (Fig. 7E), *Ilyocypris bradyi* (Fig. 7D) and *Pseudocandona parallela* (Fig. 7G). Some samples also include minor amounts of *Candona* sp., *Cypridopsis vidua*, *Darwinula stevensoni* (Fig. 7I), *Ilyocypris gibba* (Fig. 7F), *Paralimnocythere psammophila*, *Pseudocandona eremita* and *Pseudocandona marchica* (Fig. 7H; Table 1). The preservation of ostracod shells is good in all samples from Units 2 and subunits 3A to 3C, in some samples occurring as pristine calcite caparaces. Thin section analysis revealed that ostracods are also common in all indurated carbonate palustrine and lacustrine deposits within subunits 3A to 3D but similarly to gastropods, they show evidence of dissolution and/or neomorphism.

4.3.3. Charophytes

In Units 2 and subunits 3A-C, this group is represented by three different taxa: *Lychnothamnus* sp., *Chara* sp. and *Chara* cf. *molassica* var. *notata* (Fig. 7A, B, C) (Straub, 1952; Soulié-Märsche, 1989). The former two are particularly abundant in the two samples of limestone-marlstones of Unit 2. As revealed by thin sections, charophyte stems and gyrogonites are common components in the Lm-ch deposits of subunit 3C and in facies Lbf-mw and Lb-m of subunit 3D, in which they occur as reworked fragments or forming concentrations attributed to para-autochthonous charophyte meadows. In all lacustrine and palustrine deposits charophytes are affected by partial dissolution and moderate-intense neomorphism.

4.4. Mineralogy and $\delta^{13}C$ and $\delta^{18}O$ composition

In terms of mineralogical composition, calcite is the dominant phase in almost all samples, ranging between 80 and 100 % (Table S2). The single sample of chalky dolomitic marlstone (CDm) contains calcite (2 %), dolomite (79 %), palygorskite (16 %) and quartz (3 %). The second most abundant mineral phase is aragonite, whose contents varying between 4 and 20 % in 23 samples, and between 30 and 50 % in 3 samples. Most aragonite derives from tiny gastropod fragments within the matrix that could not be split off. The mineralogical analysis of 3 single gastropod specimens (samples AD-32, AD-56 and AD-115) provides aragonite contents of 32, 36 and 58 % respectively, thus documenting their aragonitic or bimineralic (aragonite+calcite) composition. Finally, it is important to note that detrital quartz is minor but present in most samples, with percentages varying between 1 and 11 % (Table S2).

Excluding the three samples with the highest aragonite content, and after correction for isotopic enrichment of dolomite and aragonite-bearing samples (see Database and methods), correlation coefficients between aragonite content and $\delta^{13}C$ and $\delta^{18}O$ are $r = +0.80$ and $r = +0.83$, respectively; in the case of calcite content are $r = -0.57$ for $\delta^{13}C$ and $r = -0.69$ for $\delta^{18}O$ (Table S2).

The $\delta^{13}C$ and $\delta^{18}O$ values of the whole sample set shows a moderate range of variation. The $\delta^{13}C$ values range from −4.54 to −8.60 ‰ VPDB (average = −6.63 ± 1–08 ‰ VPD), and the $\delta^{18}O$ from-2.64 to −6.74 ‰ VPDB (average = −5.57 ± 1.04 ‰ VPDB; Table S2 and Fig. 8). The correlation coefficient between these $\delta^{13}C$ and $\delta^{18}O$ data is $r = +0.42$ ($r = +0.39$, if uncorrected values are considered).

The average isotopic values and the correlation coefficients vary depending on sedimentary facies and their vertical stratigraphic distribution (Tables 2, 3; Fig. 9). By sedimentary facies (Table 2; Fig. 9), the most negative $\delta^{13}C$ values occur within the group of bioturbated facies (Lb-m, Lbn-wp and Lbf-mw, Lm-ip), with an average $\delta^{13}C$ of −7-48 ± 0.93 ‰ VPDB. The average $\delta^{13}C$ value of the massive bioclastic limestones (Lm-chg, Lm-ch and Lm-g(wp)) is −6.28 ± 0.95 ‰ VPDB and that of the layered gastropod limestone-marlstones (Ll-g(wp)) is −6.20 ± 1.00 ‰ VPDB, thus ca. 1.2 ‰ higher than that of the palustrine deposits. The average $\delta^{18}O$ values vary in the same order as for $\delta^{13}C$ in the three facies groups, with an average of −5.96 ± 0.60 ‰ VPDB for the bioturbated, of −5.76 ± 1.01 ‰ VPDB for the massive bioclastic and of −5.13 ± 1.12 ‰ VPDB for the layered bioclastic deposits (Table 2). The sample of facies CDm from subunit 3A (PAF-1*) is set apart due to the high dolomite content, and yielded $\delta^{13}C = -5.45$ ‰ and $\delta^{18}O = -2.80$ ‰ VPDB. The bioturbated limestone-marlstones (L-Mb) of Unit 2 show $\delta^{13}C$ values intermediate between the three other groups, and the least negative $\delta^{18}O$ values, excluding the dolomitic sample (Fig. 9). The correlation coefficients between $\delta^{13}C$ and $\delta^{18}O$ are significant and positive for the bioturbated limestones, and less significant to poor in the other three facies groups (Table 2).

The $\delta^{13}C$ values show a wide range of variability through the stratigraphic section, while $\delta^{18}O$ values only have wide variability in subunit 3A (Fig. 8). The evolutions of $\delta^{13}C$ and $\delta^{18}O$ expressed by LOESS smoothing depict oscillating curves through time, but with overall increasing $\delta^{13}C$ and decreasing $\delta^{18}O$ evolutions from subunit 3A to subunit 3D (Fig. 8). By sedimentary units (Table 3) the lowest average $\delta^{13}C$ values are those of subunits 3B and 3D. The average $\delta^{18}O$ values are higher in Unit 2 and subunit 3A, and the lowest in subunits 3B and 3C. The correlation coefficients between $\delta^{13}C$ and $\delta^{18}O$ are significant and positive for subunits 3A and 3B (Table 3).

5. Interpretation and discussion

The stratigraphic-sedimentological study of the Peña Adrian Formation revealed a lacustrine succession showing a wide range of depositional facies, a complex facies architecture and a rich and varied record of calcareous benthic biota. In the following sections, main interpretative issues concerning the calcareous biota, the significance of $\delta^{13}C$ and $\delta^{18}O$ composition and the sedimentological characterization of facies are used to build a depositional model and to discuss the evolution of the paleolake and the potential control exerted by climate and tectonism.

5.1. Environmental inferences from calcareous biota

The abundance of calcareous biota is the main compositional characteristic of the Peña Adrian lacustrine succession, particularly of the open lacustrine facies of subunits 3A-C and some palustrine intervals of Unit 2. The taxonomic determinations in such units revealed varied associations of small gastropods and ostracods, and a low-diversity, almost monospecific association of charophyte (Table 1). Most genera and species determined in the three groups have extant representatives with ecological preferences well documented in the literature, which are them useful for inferences of the ecological and physico-chemical conditions that prevailed during development of the Peña Adrian lake system.

Most taxa of the gastropod assemblage are common in numerous modern subtropical to temperate freshwater ponds and shallow lakes across northern Africa, Europe, Asia and North America. The association of small gastropods comprises both pulmonate and prosobranch aquatic taxa, which in modern lakes live adapted to shallow and well-oxygenated shallow muddy bottoms colonized by algae and macrophytes, sometimes as epiphyte components, and in which they mainly feed on living plants, degraded plant detritus and even carrion (Dillon, 2006). The dominant hydrobiid *Mercuria* sp. has been common in the western Mediterranean and Atlantic lowland freshwater records since the Miocene (Miller et al., 2022). It usually inhabits freshwater to slightly brackish ponds and shallow lakes, preferentially on densely vegetated littoral to sublittoral areas (Álvarez-Halcón et al., 2012). Different studies document that modern small hydrobiid, planorbid and

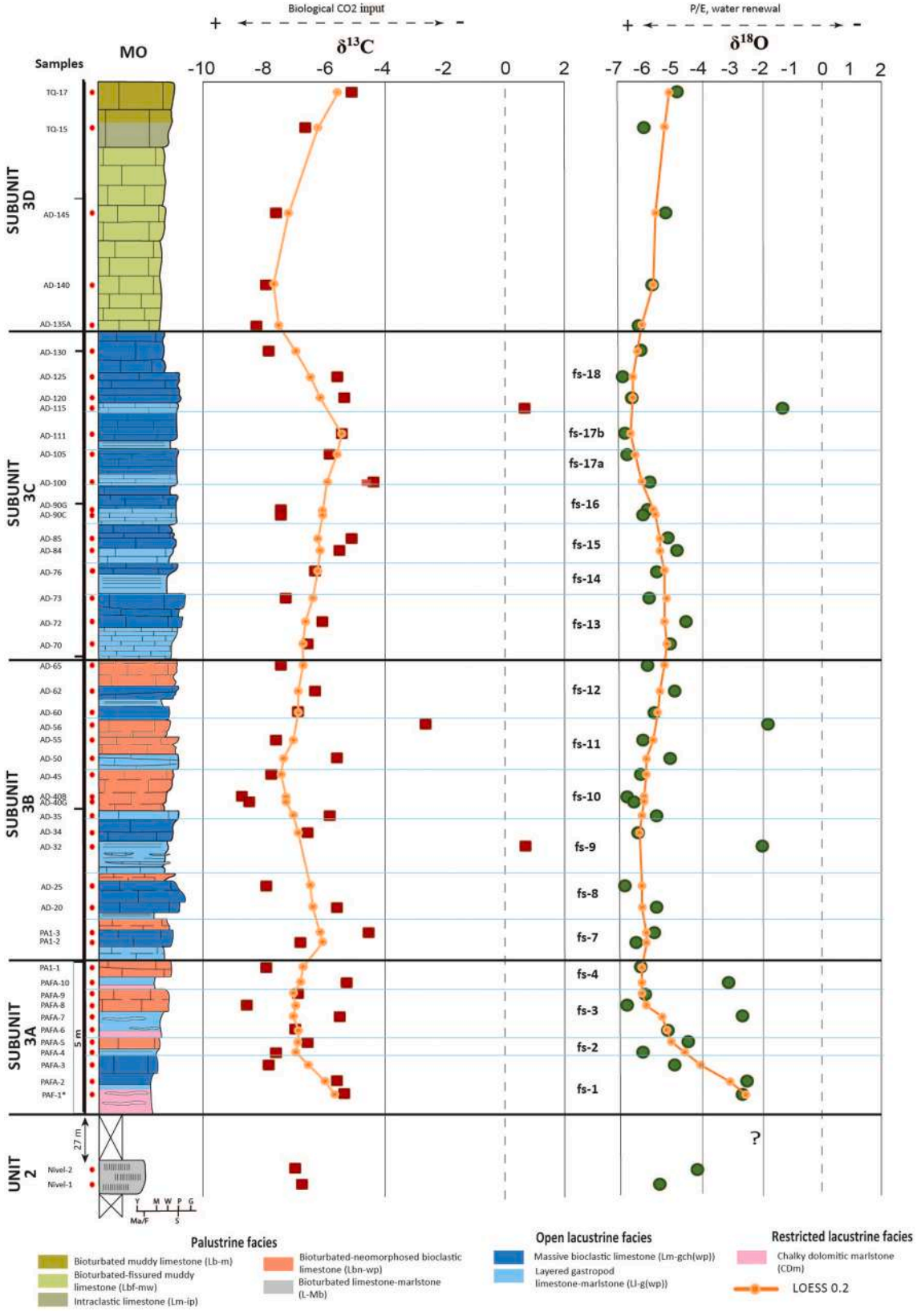

Fig. 8. Stratigraphic log from the Morro section with samples used for the isotopic evolution. The vertical evolution of $\delta^{13}C$ and $\delta^{18}O$ values (corrected for mineralogy fractions if needed, as explained in Database and methods). The relation with the biological CO_2 input, precipitation/evaporation balance and water renewal are indicated. Orange line represents smoothing through LOESS (Locally Estimated Scatterplot Smoothing).

Table 2
Average $\delta^{13}C$ ‰ (VPDB) and $\delta^{18}O$ ‰ (VPDB) values of the samples in analysed in Unit 2 and subunits of Unit 3 according to the facies types. The value of correlation coefficient (r) is indicated.

Sedimentary facies		N	δ^{13C} ‰ (VPDB)		δ^{18O} ‰ (VPDB)		Correl coef (r)	
Bioturbated-fissured limestone	Lb-m	1	−5.16	−7.48 ± 0.93	−5.01	−5.96 ± 0.60	–	0.75 (N = 14)
	Lbn-wp	10	−7.71 ± 0.71		−6.09 ± 0.62		0.84	
	Lbf-mw	3	−7.82 ± 0.3		−5.82 ± 0.47		–	
	Lm-ip	1	−6.61		−6.12		–	
Massive bioclastic limestone	Lm-chg	3	−6.27 ± 1.33	−6.28 ± 0.95	−6.50 ± 0.28	−5.76 ± 1.01	–	0.13 (N = 18)
	Lm-ch	2	−5.14 ± 0.72		−5.69 ± 0.07		–	
	Lm-g(wp)	13	−6.45 ± 0.84		−5.60 ± 1.12		0.27	
Layered gastropod limestone-marlstone	Ll-g(wp)	13	−6.20 ± 1.00	−6.20 ± 1.00	−5.13 ± 1.12	−5.13 ± 1.12	0.48	
Chalky dolomitic marlstone	CDm	1	−5.45	−5.45	−2.80	−2.80	–	
Bioturbated limestone-marlstone	L-Mb	2	−6.71 ± 0.21	−6.71 ± 0.21	−4.92 ± 0.89	−4.92 ± 0.89	–	

Table 3
Average $\delta^{13}C$ ‰ (VPDB) and $\delta^{18}O$ ‰ (VPDB) values of the samples analysed according to stratigraphic units (Unit 2 and subunits 3A-3C). The value of correlation coefficient (r) is indicated.

Sedimentary unit	N	d13C ‰ (VPDB)	d18O ‰ (VPDB)	Correl coef (r)
Subunit 3D	5	−7.05 ± 1.2	−5.72 ± 0.53	0.65
Subunit 3C	15	−6.17 ± 0.98	−5.89 ± 0.67	0.02
Subunit 3B	16	−7.02 ± 1.04	−5.97 ± 0.53	0.83
Subunit 3A	11	−6.57 ± 1.1	−4.89 ± 1.50	0.66
Unit 2	2	−6.71 ± 0.21	−4.92 ± 0.89	–

Lymnaeidae gastropods mainly attain large populations in neutral to slightly alkaline calcium-rich waters with averaged annual temperatures over 12 °C (see Tessier et al., 2004; Dillon, 2006; Neubauer, 2024 and references therein).

Concerning the ostracod association, the dominant taxon *Cypris bispinosa* is characteristic of many shallow ponds and lakes with submersed and riparian vegetation since the Pliocene (Meisch, 2000), as well as in temporary fresh or slightly saline waters (<3.6 ‰) (Martín-Rubio, 2003). *Darwinula stevensoni* is usually indicative of permanent water systems, such as rivers and shallow lakes with organic-rich bottoms and variable current activity (Meisch, 2000). According to Ninemets (1999), a persistent occurrence of *Ilyocypris bradyi*, as found within subunits 3A-C, likely points to conditions of moderate to high energy. *Darwinula stevensoni* and *Ilyocypris bradyi* occur and attain higher concentrations in the three samples collected in subunit 3C, which is thought to represent the stage of maximum expansion of shallow open conditions through the studied lacustrine system (see below).

Studies of charophyte communities from modern environments document that representatives of the genera *Lychnothamnus* sp. and *Chara* sp. preferentially flourish in ponds and shallow lakes with slightly alkaline waters recording marked seasonality and repeated wet and drying stages (Krause, 1997; Casanova et al., 2003). Similar conditions have been inferred for the *Lychnothamnus* sp. rich deposits of the Late Miocene La Cerdanya Lake system (Martín-Closas et al., 2006), largely contemporary to the Peña Adrian Formation. In turn, *Chara* cf. *molassica* var. *notata* is the only taxon identified in the samples from subunits 3A to 3C. It was a very common species in Chattian-Tortonian wetland and lacustrine systems developed across Europe and the Middle East, including the Tajo, Ebro and Vallès-Penedès lacustrine basins of the Iberian Peninsula (Sanjuan et al., 2022). According to these authors, Ch. *molassica* var. *notata* developed in a broad ecological spectrum from palustrine to shallow lacustrine environments of fresh to slightly brackish waters.

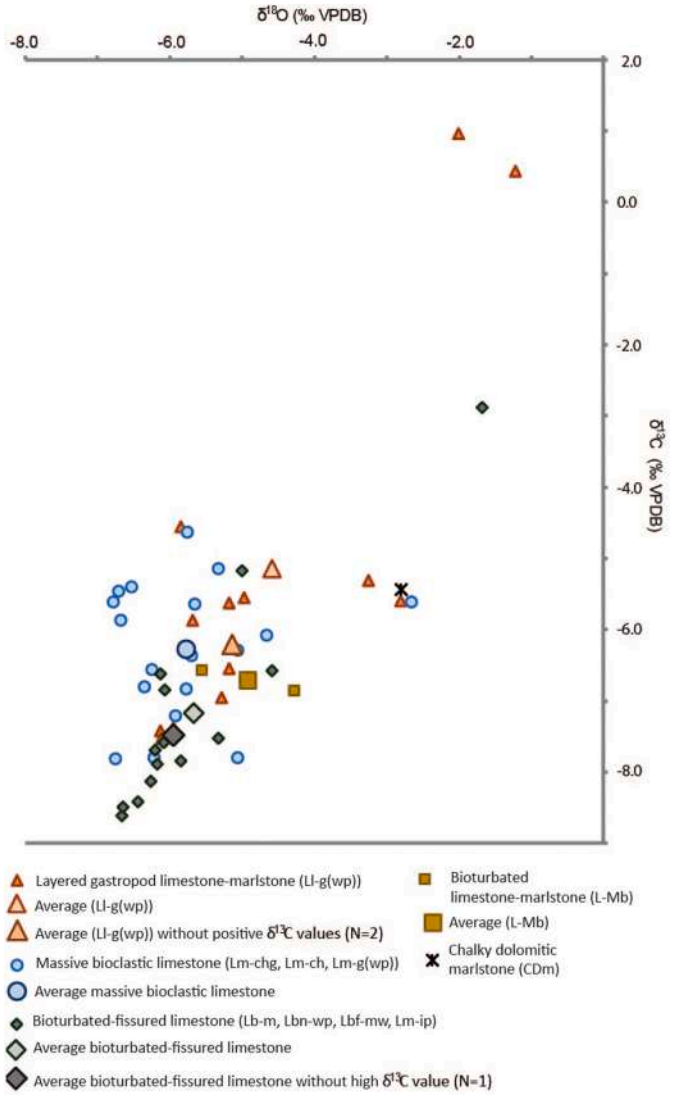

Fig. 9. Plot of $\delta^{13}C$ versus $\delta^{18}O$ (‰ VPDB) according to facies types. Values in Table 2.

5.2. Significance of $\delta^{13}C$ and $\delta^{18}O$ composition of the carbonate facies

5.2.1. General considerations

In closed-lake systems dominated by chemical precipitation, as was the case of the Peña Adrian system, water level variations are mostly related to the balance between water input, via groundwater and/or surface supply (together reflecting the precipitation), and evaporation (P/E ratio) (Arenas et al., 1997; Gierlowski-Kordesch, 2010; Deocampo, 2010). The lake carbonate $\delta^{18}O$ variations can be interpreted in terms of varying P/E ratios or lake water renewal (Talbot, 1990; Leng and Marshall, 2004). Temperature influences the $\delta^{18}O$ composition of air and water (Lachniet, 2009). However, interpreting temperature variations from $\delta^{18}O$ values of carbonates formed in closed lakes is not

straightforward, because of the superposed water lake ^{18}O-enrichment caused by evaporation effects (Valero Garcés et al., 2000; Arenas et al., 2024). Aquifers held in marine-carbonate rocks, as is the study case, provide water with varying $\delta^{13}C$ composition depending on parameters such as recharge frequency and in-aquifer temperature. Yet the ^{12}C-enriched CO_2 of biological origin greatly contributes to the $\delta^{13}C$ signature of meteoric water. The lake carbonate $\delta^{13}C$ variations can be explained by changes in humidity and biota development, atmospheric CO_2 equilibration and biological processes in the lake (Kelts and Talbot, 1990; Leng and Marshall, 2004).

5.2.2. Interpretation of the isotopic values of the Peña Adrian lake system

The $\delta^{13}C$ and $\delta^{18}O$ values of the analysed carbonate samples are indicative of freshwater carbonate environments with relatively high CO_2 input of biogenic or soil origin and variably affected by evaporative effects (Platt, 1989; Talbot, 1990; Leng and Marshall, 2004; Deocampo, 2010). In such conditions, the variability in $\delta^{13}C$ values can be interpreted in terms of humidity, as well as related to plant activity and soil-related compositional transformations (Platt, 1989; Armenteros et al., 1997). In general, the $\delta^{13}C$ values of samples from palustrine deposits in the study area are more negative and have higher dispersion than those from the open lacustrine deposits (Fig. 9). This variation may indicate the different development of vegetation cover in and around the lake, with changing influence of soil-derived CO_2, which would be higher in the palustrine environment (facies Lb-m, Lbn-wp, Lbf-mw and Lm-ip, and bioturbated limestone-marlstones (L-Mb) of Unit 2). Poor soil-derived CO_2 input would have contributed to the carbonate $\delta^{13}C$ of dolomite marly environment (facies CDm). The $\delta^{18}O$ values suggest variable P/E ratio, which would be similar during deposition of palustrine and massive bioclastic facies, reflecting poor evaporation effects (Talbot, 1990; Deocampo, 2010; Moreau et al., 2023). Slightly higher average $\delta^{18}O$ values of the layered bioclastic facies might suggest overall slightly higher evaporation; however, provided the isotopic data dispersion of facies Ll-g(wp) (Table 3; Fig. 9), the latter might also reflect similar P/E conditions to those of the massive bioclastic facies at certain moments. The $\delta^{18}O$ values of carbonate deposits in Unit 2 (L-Mb) suggest similar to slightly higher P/E conditions than those of above mentioned facies. In contrast, the high $\delta^{18}O$ value of the dolomitic facies (subunit 3A) fits intense evaporation in shallow lake conditions, leading to dolomite precipitation (Arenas et al., 1997; Valero-Garcés et al., 2000). Moreover, these conditions favoured palygorskite formation (non-detrital crystals as revealed by SEM observations). Together these features support a primary origin of dolomite.

5.3. Characterization of the lacustrine depositional environment

The sedimentological and mineralogical results indicate that the different sedimentary facies formed in distinct depositional and hydrological conditions, driven by lake water level, sediment supply, biological development and hydrodynamics. The three main facies associations (FA2-FA4), representing distinct lacustrine environments, are characterized as follows.

5.3.1. Open lacustrine facies association (FA2)

Two main groups fit this association: i) massive bioclastic limestones, which include three variants based on biological components (gastropod wackestone-packstone (Lm-g(wp)), charophyte mudstone-wackestone (Lm-ch) and charophyte-gastropod wackestone-packstone (Lm-chg)), and ii) layered bioclastic limestones (layered gastropod limestone-marlstone (Ll-g(wp))). The deposits of FA2 make the bulk of subunits 3A to 3C and are characteristic in the central outcrops of the Peña Adrian Formation between Falla and Depósito sections (Fig. 2A).

The massive bioclastic limestones indicate shallow and open lacustrine settings affected by variable energy processes and sediment transport and supply. Facies Lm-ch most likely developed in littoral zones, with calm and well-oxygenated waters favourable for the proliferation of charophyte meadows, as described by Villalba-Breva and Martín-Closas (2013) in the Upper Cretaceous carbonates of the Southern Pyrenean Basins. Facies Lm-chg, with high amounts of molluscs, shell fragments and quartz grains, likely record the effects of occasional inflows transporting fine clastic particles, as well as bioclasts from adjacent littoral zones (Sturm and Matter, 1978; Muniz, 2013).

The gastropod-rich deposits (Lm-g(wp)) likely document stages, or lake zones, of reduced to absent clastic input and, thus, represent the lake areas evolving under the most stable conditions in terms of water composition (i.e., salinity), oxygen levels, temperature and nutrient availability. The interbedded discontinuous coquina layers probably indicate reworking and concentration of bioclastic components caused by moderate energy currents associated with storms and wind-driven wave activity (Carvalho et al., 2000; Jahnert et al., 2012). These currents would transport the bioclastic components to nearby zones above and below the fair-weather wave base (Muniz, 2013). Similar discontinuous layers of fresh to brackish-water mollusc coquinas have been described in the Early Cretaceous Pre-Salt lacustrine successions of the Campos Basin (Carvalho et al., 2000; Thompson et al., 2015; Oliveira et al., 2019), the Santos Basin (Carlotto et al., 2017) and the Sergipe-Alagoas Basin (Kinoshita, 2010; Tavares et al., 2015), as well as in Barremian lacustrine limestones on the west African margin (Hassan et al., 2016).

The layered deposits (Ll-g(wp)) developed in shallow open lacustrine areas, having similar features to those of the massive bioclastic carbonate deposits, but additionally received intermittent inflow carrying suspended fine clastic sediment and plant debris from the marginal zones. These sediment inputs were associated with fluvial discharge periods, likely leading to rise in lake level (Arenas and Pardo, 1999; Alonso-Zarza and Wright, 2010). The presence of discontinuous coquina layers, together with scoured surfaces, give evidence of episodic reworking and redistribution of bioclasts by wind-induced storms (Sturm and Matter, 1978; Glenn and Kelts, 1991; Platt and Wright, 1992; Sáez et al., 2007; Gierlowski-Kordesch, 2010). Spatial changes in the intensity of erosion, transport and accumulation of bioclasts and fine carbonate and silicic clastic sediment due to varying current strength, produced irregular bottom topography, bed amalgamation and the lateral pinch and swell bed patterns that characterize many deposits formed of layered gastropod limestone-marlstones (Fig. 5E). Similar deposits have been described in the Miocene limestones of the Lake Sinj, Croatia (Mandic et al., 2008), where gastropod coquina layers and fine coal seams are interspersed in a shallow, calm and freshwater lacustrine environments with infrequent higher energy storm events.

Aside of their great abundance, the good preservation of gastropods of aragonitic and bimineralic composition is characteristic of both Lm-g(wp) and Ll-g(wp) open lacustrine facies. It is likely that a taphonomic effect favoured by the low sulphide activity of freshwaters and the rapid burial of shells due to enhanced bioclastic production-accumulation and recurrent high-energy processes can explain the good preservation of gastropods, as was inferred by Wright et al. (2018) for some molluscan faunas in the Upper Jurassic of Portugal. The common presence of disseminations of iron sulphides (pyrite?) in all open lacustrine deposits suggests dominant low oxygen levels at the time of early burial and lithification (Armenteros, 2010). The amounts of comminute coalified plant remains reflect recurrent inflows from adjacent palustrine and emerged areas and later coalification (Cabrera and Sáez, 1987; Mandic et al., 2008).

5.3.2. Palustrine facies association (FA3)

This association comprises five distinct facies types: bioturbated limestone-marlstone (L-Mb), rhizogenic calcrete (Calc), bioturbated-neomorphosed bioclastic limestone (Lbn-wp), bioturbated-fissured muddy limestone (Lbf-mw), intraclastic limestone (Lm-ip) and bioturbated muddy limestone (Lb-m) (Table S1). Facies Ma and Calc predominate in Unit 2, facies Lbn-wp predominate in subunits 3A to 3B, and the last three facies (Lbf-mw, Lbn-wp, and Lm-ip) comprise subunit 3D

(Fig. 3).

The bioturbated limestone-marlstones (L-Mb) represent vegetated environments that received fine siliciclastic sediment (quartz and clays) through semi-continuous surface water inputs and that experienced episodic subaerial exposure and desiccation. In favourable conditions, these could be inhabited by gastropods, charophytes and ostracods. The presence of discontinuous sub-metric thick rhizogenic calcretes (Calc facies) indicates colonization of land plants with coeval carbonate cementation during episodes of prolonged subaerial exposure (Armenteros and Daley, 1998; Alonso-Zarza and Wright, 2010).

The bioturbated-neomorphosed bioclastic limestones (Lbn-wp) are representative of littoral bioclastic lime mud-depositing areas, which hosted hygrophilous plants and experienced repetitive water level changes. The latter caused episodic subaerial exposure, desiccation and cracking (Huerta, 2006; Alonso-Zarza and Wright, 2010). These processes together with plant activity overprinted the initial lime mud features. As documented by Sommer et al. (2006), Bustillo et al. (2002), and Bustillo (2010), the precipitation of silica nodules can be associated to microbial activity in a scenario of evaporation and enhanced by the plant activity. Similar palustrine facies with root traces and silica nodules occur in Middle Miocene deposits of the Ebro basin (Vázquez-Urbez et al., 2013), and in Upper Triassic deposits of southwest USA (Tanner, 2000).

The bioturbated-fissured muddy limestones (Lbf-mw), intraclastic limestones (Lm-ip) and bioturbated muddy limestones (Lb-m) that form subunit 3D fit laterally-extensive palustrine environments affected intermittently by subaerial exposure, desiccation and recurrent reflooding (Freytet and Plaziat, 1982; Platt, 1989; Freytet and Verrechia, 2002; Alonso-Zarza and Wright, 2010). Plant colonization aided the development of cracking and brecciation, features that are better represented in the bioturbated-fissured muddy limestones (Lbf-mw). The intraclastic limestones (Lm-ip) also suggest episodes of reworking by currents that carried fine siliciclastic sediment (Freytet, 1973; Freytet and Plaziat, 1982; Alonso-Zarza et al., 1992; Freytet and Verrechia, 2002). Similar facies comprising a variety of pedogenetic features have been described in the upper Eocene Bembridge Limestones, southern England (Armenteros and Daley, 1998), in the Campanian Fortanete Formation of the Maestrazgo basin, NE Iberia (Torromé et al., 2023) and in the modern-day Florida Everglades (Platt and Wright, 1992). Additionally, the dense networks of subvertical root traces and fissures with varied internal sediment, typical of Lb-m facies, resemble pedogenic pseudo-microkarst features (Freytet and Plaziat, 1982) associated with active colonization of land plants over aggrading palustrine areas recording episodes of prolonged subaerial exposure.

The dissolution and/or moderate-intense neomorphism affecting the bioclastic fraction and matrix in most palustrine deposits are common early diagenetic processes in palustrine environments (Armenteros, 2010). Disseminations of iron sulphides occur in most muddy palustrine deposits, and mottles and haloes of iron oxides mainly formed around root traces and desiccation fissures. The coexistence of both iron-rich phases in many beds is likely indicative of alternating oxic and anoxic conditions following water level fluctuations (Freytet and Plaziat, 1982). In the case of gastropods, the increased salinity after evaporation and the acidity associated to plant activity may have controlled the preservation or dissolution of aragonitic or bimineralic shells (Alonso-Zarza and Wright, 2010; Wright et al., 2018). In freshwater and brackish environments with low sulphate concentrations, the preservation potential of primary biogenic aragonite is relatively high across the *taphonomically active zone* (*TAZ*) (Wright et al., 2018), mainly due to a reduced sulphide activity (e.g. Sanders, 2003; Cherns and Wright, 2011; Wright et al., 2018). By contrast, in the *final burial zone* (*FBZ*) of the same authors, the aragonitic and bimineralic shells may in turn be actively dissolved, providing distinct moldic porosity or recording intense replacement by sparite.

5.3.3. Restricted facies association (FA4)

Chalky dolomitic marlstone (CDm) is the only facies in FA4 and is exclusive to subunit 3A. The lack of lamination and the dominant fine crystalline texture of the chalky dolomitic deposits indicate dolomite precipitation in a shallow lacustrine setting, subjected to water restriction and with intense evaporation, likely associated with episodes of water level drops. In these conditions, the lake water would have attained higher salinity, with Mg/Ca ratios favourable for the precipitation of both high-Mg calcite and dolomite (almost stoichiometric) (Tucker and Wright, 1990; Calvo et al., 1995; Arenas et al., 1997; Rodríguez-Aranda and Calvo, 1998; Armenteros, 2010). Similar dolomite facies have been described by Cañaveras et al. (2020) in the Late Miocene deposits of the Madrid Basin (Spain) and in the Pliocene of La Roda (García del Cura et al., 2001). The presence of palygorskite in association with the dolomite reinforces a lacustrine setting dominated by evaporative conditions (Arostegui et al., 2011).

5.4. Facies sequence arrangement and sedimentary facies model

According to sedimentological features and stratigraphic arrangement the studied deposits of the Peña Adrian Formation can be integrated in the generic model of low-energy shallow lake systems with ramp-shaped margins established by Platt and Wright (1991). Within low-gradient systems, water level variations produce extensive migrations of lakeshores and cause the formation of facies sequences of different scales, reflecting shallowing and deepening processes (Arenas and Pardo, 1999), as those described below. Based on the sedimentological and hydrological significance of the afore described facies and facies associations, up to eighteen facies sequences, decimetre to metre thick, can be distinguished through Unit 3 (fs-1 to fs-18 in Fig. 3). These sequences represent the vertical superposition of laterally related environments, mostly following shallowing upward processes. These are particularly evident in the correlation scheme of subunits 3A to 3C (Fig. 3).

In subunits 3A to 3C, the most common facies sequence consists of 1–3 m thick packages of sharp-based layered gastropod limestone-marlstones (Ll-g(wp)) in gradual vertical transition to massive gastropod limestones (Lm-g(wp)), i.e., fs-1 to fs-18 (Figs. 3, 4). Significantly, sequences fs-1, fs-3 and fs-4 also include a distinct basal interval of chalky dolomitic marlstone (CDm), representative of stages of increased restriction and evaporation across the lacustrine basin, which is consistent with the lack of fossil remains in CDm. Additionally, several sequences in subunits 3A and 3B comprise basal and/or capping intervals and interbedded deposits indicative of littoral and palustrine setting (Lm-ch, Lm-chg and Lbn-wp), particularly best developed in the Morro section (Figs. 3, 4). Sequences formed of capping intervals bioturbated-neomorphosed limestones (Lbn-wp) are noteworthy (Fig. 6B). They exemplify the establishment of palustrine conditions over previous littoral deposits, as a result of lake level lowering, which would cause marked shoreline migrations offshore.

In contrast, subunit 3D does not show clear facies sequences. Along the Morro-Depósito outcrops, from base to top, facies occur as follows: bioturbated-fissured muddy limestones (Lbf-mw), intraclastic limestone (Lm-ip) and bioturbated muddy limestone (Lb-m). A similar vertical succession is identified in all outcrops located further southeast (Cantera and San Miguel sections), a fact documenting the widespread shallowing and final desiccation across most, if not all, the studied lacustrine system.

A sedimentary facies model is proposed to summarize the distinct depositional and hydrologic characteristics corresponding to three lake level situations, as represented by subunits 3A to 3C (Fig. 10). During low lake-level conditions (Fig. 10A) episodes of enhanced evaporation and restriction occur, similar to the episodes of underfilling and marked negative water balance stablished by Bohacs et al. (2000) during the evolution of closed and semi-closed lake basins. These conditions are recorded at the base of three facies sequences of subunit 3A. During

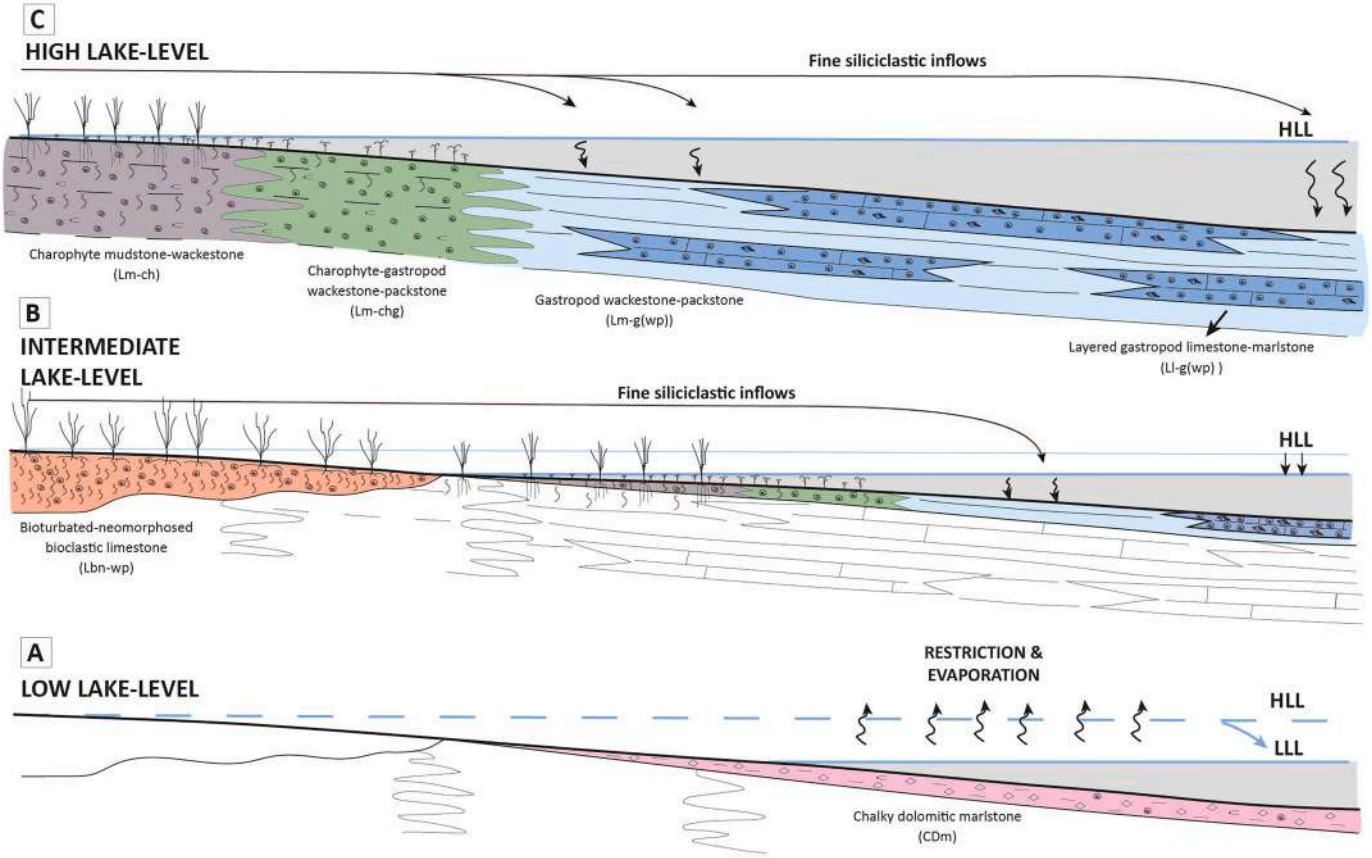

Fig. 10. Detailed depositional facies model for subunits 3A to 3C. Low lake-level: low water level with high evaporation represented by subunit 3A. Intermediate lake-level: oscillating water level between low and high, with high colonization by plants in the littoral and eulittoral areas during water drops, represented by subunits 3A and 3B. High lake-level: high water level, with fine siliciclastic inflows, largest lake expansion and extension of open lacustrine facies deposition (subunit 3C).

periods of high lake-levels (Fig. 10C), well recorded in subunit 3C, the most stable and favourable conditions for calcareous biota occur, with abundant gastropods and charophyte meadows. In conditions of intermediate lake-level (Fig. 10B), bioturbated-neomorphosed bioclastic limestones (Lbn-wp) predominate, covering eight different sequences within subunits 3A and 3B in almost marginal zones that document stages of basinward lakeshore migration, with the establishment of palustrine conditions on areas corresponding to previous littoral to open lacustrine deposits (Arenas and Pardo, 1999).

5.5. Evolution of depositional environments through time

The vertical variation in the type and distribution of dominant facies in each unit allows the differentiation of three consecutive stages through the large-scale evolution of the lacustrine systems (Fig. 11).

The first stage corresponds to Unit 2 and is defined by the establishment of a muddy vegetated palustrine area that aggraded and expanded progressively towards the basin margins under a semi-continuous supply of fine siliciclastic sediment. This palustrine area attained a minimum width of ca. 3.5 km. Within the bioclastic limestone-marlstone succession, the abundance of *Cypris bispinosa*, *Lychnothamnus* and *Chara* charophyte taxa, and the presence of a *Mercuria* dominated gastropod group support the existence of well-oxygenated freshwater conditions. Studies on modern wetlands document that *Lychnothamnus* and *Chara* mainly flourish in ponds and shallow lakes that record seasonal-induced wet and drying stages (Krause, 1997; Casanova et al., 2003). Similar conditions have been also inferred for the last filling stage of the late Miocene La Cerdanya siliciclastic-dominated lake (Martín-Closas et al., 2006), a system largely coeval to the Peña Adrian Formation.

Subunits 3A to 3C altogether characterize the second evolutionary stage, during which lacustrine and palustrine facies attained greater development (Figs. 10, 11). From an initially low lake-level with greater evaporation and precipitation of dolomite (subunit 3A), the lake evolved to freshwater conditions, experiencing and overall expansion through time. In these freshwater conditions, repetitive water level changes caused extensive shoreline migrations and produced up to eighteen shallowing facies sequences (Fig. 3). High lake-level prompted high proliferation of calcareous biota and layered deposits offshore, whereas relative lowering water table to intermediate lake-levels led to formation of extensive palustrine areas with abundant vegetation on the margins. The lowest $\delta^{18}O$ values of subunits 3B and 3C suggest higher P/E ratio than during deposition of subunit 3A, which is consistent with decreasing salinity and the expansion of the lake body, reaching its best development during deposition of subunit 3C (Fig. 8, Table 3). The slight rise of average $\delta^{13}C$ value in subunit 3C respect to previous subunits (Table 3) matches a decrease in paleosol development and the expansion of open lacustrine conditions during deposition of subunit 3C.

The last stage, recorded by subunit 3D (Fig. 11), is dominated by a laterally-extensive palustrine area. These deposits represent vegetated palustrine environments affected intermittently by subaerial exposure, desiccation and recurrent reflooding. Evidence of root activity is more evident in the uppermost interval, which exhibits dense networks of subvertical to irregular pseudo-microkarst features (Freytet and Plaziat, 1982). The general vertical facies arrangement characterizes a phase of intermittent vertical aggradation that culminated with the final filling of the Peña Adrian lacustrine basin. Though based on five values, the average $\delta^{13}C$ value of subunit 3D (Table 3) agrees with soil

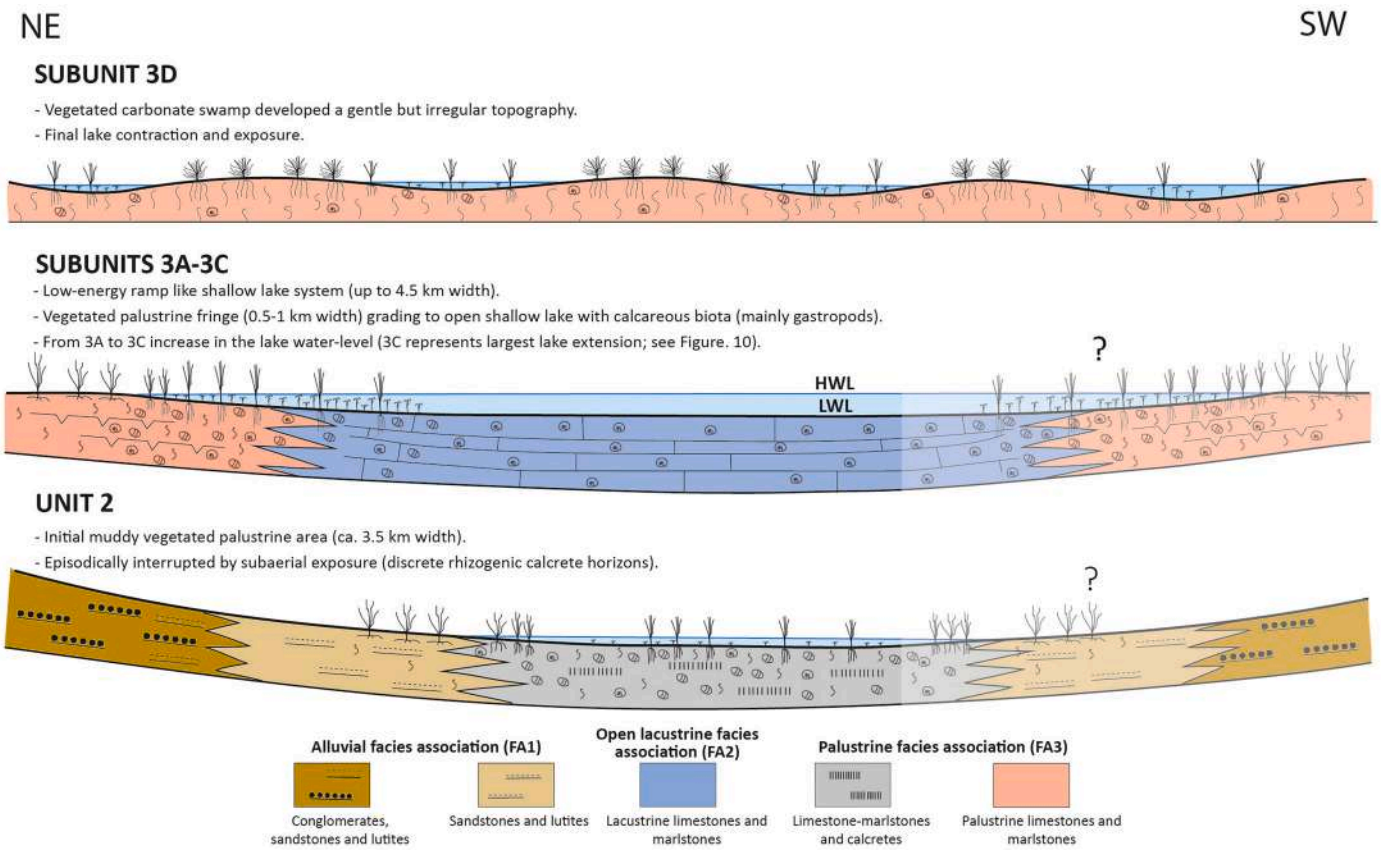

Fig. 11. Evolutionary stages through time. Unit 2) Middle to distal alluvial deposition grading into palustrine pond with abundant charophyte and hygrophilous vegetation. Subunits 3A-C) freshwater shallow lake surrounded by palustrine fringe. Subunit 3D) Palustrine wetland with intermittent changes in the water level and consequent subaerial exposure and colonization by plants.

development, and an overall decline in humidity and a decrease in P/E rates during this phase respect to previous ones is suggested by both C and O data (Fig. 8). The general depositional setting inferred is that of a km-wide vegetated carbonate swamp that developed a gentle but irregular topography, in a similar scenario to the series of sloughs, prairies and hummocks described in the modern Florida Everglades by Platt and Wright (1992).

5.6. *Tectonic setting and climate control on sedimentation*

Local-regional tectonism and climate are major factors influencing the evolution of lacustrine systems (i.e. Kelts and Talbot, 1990; Carroll and Bohacs, 1999; Gierlowski-Kordesch, 2010; Benavente and Bohacs, 2024). In terms of tectonic context, the Peña Adrian paleolake developed during an interval of relative quiescence along the southern Basque Pyrenees, following the main phases of deformation, uplift and active denudation that defined Oligocene to Middle Miocene times. Despite these general conditions, there is unambiguous evidence documenting that differential subsidence persisted in local areas along the SPTF, associated to local thrust overload, halokinetic readjustment of detached Triassic salts and extensional faulting, allowing the creation of several small depressions with Miocene to Pliocene alluvial-lacustrine sediment fill (see Riba and Jurado, 1992; Cortés-Gracia and Casas-Sainz, 1997; Pujalte et al., 2002; Frankovic et al., 2016; Valenzuela et al., 2023; Mirumbrales-Ayllón et al., 2023). The Tortonian Peña Adrian Formation represents the fill of one of such small endorheic depressions along the southern margin of the Miranda-Trebiño piggy-back basin. The studied alluvial-lacustrine succession overlies unconformably folded and thrusted strata of its lower Oligocene infill and locally rests directly onto the Cretaceous-Paleocene substrate, a stratigraphic configuration documenting a long phase of uplift and active denudation before its deposition. The composition of the basal alluvial conglomerates (Unit 1) reveals a range of potential source areas, including the Cretaceous to Paleocene rocks forming the high reliefs of the SPTF to the west, south and southeast of the study area, and the Lower-Middle Miocene siliciclastic and carbonate series exposed to the north and northeast. The stratigraphic reconstruction and the detailed outcrop analysis of the Peña Adrian Formation do not provide clear evidence of coeval tectonism during its deposition, such as synsedimentary faulting, slumping or growth strata relationships. The only internal stratigraphic feature indicative of potential tectonic deformation is the onlap geometry described by facies sequences fs-5 and fs-6 over fs-4 along the outcrops between the Depósito and Morro sections (Fig. 3). The actual significance of this feature is difficult to establish with the available information as it might also result from local changes in accommodation and/or sediment distribution patterns. Instead, the erosional surface capping the Peña Adrian succession, only observable in the Cantera section (Fig. 2A), the associated hiatus and present-day southward tilting and local faulting affecting the formation attest to renewed tectonic activity during the latest Miocene to modern times.

On the other hand, the sedimentological attributes, stacking patterns and the depositional evolution inferred for the Peña Adrian lacustrine sediments document a depositional history influenced by changes in paleohydrological conditions potentially associated to local and regional climate control operating at different temporal scales. At the smaller scale, the carbonate intervals with authigenic calcite, dolomite and palygorskite (the basal chalky dolomitic marlstones-CDm in facies sequences fs-1, fs-3 and fs-4) document several short-lived episodes of marked drop in P/E ratios and water inflow, likely associated to phases of increasing aridity and basin restriction, which are reflected by

increased $\delta^{18}O$ values. At a larger scale, the distinct sequential ordering of the littoral to open lacustrine deposits in subunits 3A to 3C, facies sequences fs-1 to fs-18, also sustain a series of successive short-term changes in lake levels of potential climatic origin. The lateral extent, regular thickness and repetitive character of these m-thick units resemble the precession-driven sedimentary cycles identified in other Miocene to Pliocene continental basins, such as the lacustrine lignite-marl sequences of the Ptolemais basin in Greece (Steenbrink et al., 1999) and the distal alluvial-lacustrine and palustrine-lacustrine sequences in the Iberian Calatayud-Daroca and Teruel basins (Abdul Aziz et al., 2000; Abels et al., 2009; Ezquerro et al., 2014). Nonetheless, in absence of accurate age constraints, any interpretation of the characteristic m-thick open lacustrine units of the Peña Adrian Formation in terms of astronomical climatic control must remain tentative.

Finally, the overall trend of lake expansion and contraction with the three distinct depositional stages described by the lacustrine succession, seems to trace a long-term hydrological cycle also potentially related to climate variations, probably aided by the local tectonic regime. This large-scale depositional cycle involved the foundation and progressive enlargement of a shallow palustrine to lacustrine basin as a result of gradual increasing water inflow and storage, during deposition of Units 2 and subunits 3A-C, followed by a comparatively faster contraction with final exposure, exemplified by subunit 3D (Fig. 11). In terms of climate, the Late Miocene and Pliocene were defined globally by a gradual change to drier and cooler conditions, a trend well recorded in marine sediments and in numerous continental successions by changes in stable isotopes, micro- and macro-vertebrate associations and dominant land vegetation (Steinthorsdottir et al., 2020). In Europe, a series of wetter and drier climatic periods have been identified during the Late Miocene and Pliocene based on rainfall estimations from paleontological and geochemical records (i.e. van Dam, 2006; Böhme et al., 2008; Ezquerro et al., 2014), although there is still no major consensus in the number, intensity and time span of such hydrological stages and their potential link with regional and local paleotemperature estimates (for a recent discussion, see Ezquerro et al., 2022). According to precipitation estimations for central-eastern and southwestern Europe, Böhme et al. (2008, 2011) recognize two main stages of wetter (washhouse) conditions interspersed with drier periods during the Tortonian, at least outlining two complete cycles of drier-wetting-drier conditions that they correlate with marine isotopic stages, tectonic events and major paleocirculation changes at the scale of the Atlantic and Indian oceans. Without excluding the local tectonic control, the large-scale evolution of the Peña Adrian lacustrine system might respond to one of such major paleo-precipitation cycles, given its paleogeographical position close to the Bay of Biscay and thus open to North Atlantic influences. The interpretation of the potential record of a major Tortonian climate-influenced depositional cycle in the Basque Pyrenees based on the Peña Adrian paleolake is reinforced by the occurrence of coeval lacustrine carbonate successions in the same domain as, for example, the unnamed gastropod-rich limestones preserved on the northeastern tip of the Miranda-Trebiño basin (Davó et al., 1978) and the Oko Limestones infilling the fault-bounded Ancin-Murieta trough, some 70 km to the east of Peña Adrian (Valenzuela et al., 2023).

5.7. *The Peña Adrian paleolake model: comparison with ancient and modern examples*

The reconstruction of the Peña Adrian lacustrine system provides a depositional model and basin characteristics that according to Benavente and Bohacs (2024) are representative of a transitional system between semi-permanent freshwater ponds and small lakes. In terms of facies types and stratigraphic arrangement, the Peña Adrian model fits quite well in the category of low-energy shallow carbonate lakes with ramp margins established by Platt and Wright (1991). This type of systems is distinguished by relatively wide palustrine fringes recording semi-continuous small-scale water level oscillations that towards the basin centre grade to more regular littoral and open lacustrine areas with variable vegetation cover and bioclastic production that eventually converge into pelagial zones. The specific attributes of shallow, low-gradient lacustrine systems, however, may vary considerably depending on the size, physiography and the hydrological, tectonic and climatic conditions that prevailed during their development. In the Peña Adrian system a major spatial and temporal variability of the palustrine areas is revealed through comparison of the sedimentological features, extent and inferred environmental conditions of the siliciclastic-influenced limestone-marlstones of Unit 2 (evolutionary stage 1), the strongly bioturbated marginal limestone intervals characteristic of subunits 3A and B (stage 2) and the different types of intraclastic, bioturbated and fissured limestones within the laterally-extensive subunit 3D (stage 3). Most differences among these palustrine ensembles are associated to variations in the frequency and intensity of subaerial exposure, pedogenesis and plant activity, giving way to the wide range of physical, textural and mineralogical diagenetic modifications observed in the Peña Adrian deposits, well documented in numerous examples of ancient palustrine carbonates (i.e. Freytet and Plaziat, 1982; Alonso-Zarza and Wright, 2010; Armenteros, 2010; Platt and Wright, 2024 and references therein).

Apart from its palustrine deposits, the Peña Adrian system stands out by the high abundance of benthic calcareous biota, most particularly of freshwater gastropods. They are characteristic in almost all open lacustrine deposits of subunits 3A to 3C, which characterize the stage of maximum extent and facies differentiation of the paleolake system. Freshwater gastropods are very abundant in all massive (Lm-g(wp)) and layered (Ll-g(wp)) open lacustrine lithofacies and in the detail occur forming two types of bioclastic accumulations. The dominant type is limestone beds and layers of wackestone to packstone texture, showing good lateral continuity along 10's m although with common amalgamation and pinch and swell patterns. These limestones mostly include well-preserved small gastropods, all dispersed within an ungraded fine-grained to microbioclastic matrix with common presence of bioturbation traces. These characteristics point to an extensive autochtonous biocenosis representative of a shallow low energy open lake area. The abundance of gastropods in almost all beds representative of these shallow open areas characteristic of the evolutionary stage 2 mainly results from the confluence and persistence of highly favourable physico-chemical conditions (temperature, pH, alkalinity, Ca concentrations) and the extensive development of macrophyte-algal cover providing both food and refuge for the mollusc community. Similar gastropod-rich facies were common in other Cenozoic paleolakes, such as in the upper Eocene Bembridge Limestone (Armenteros et al., 1997), the Lower-Middle Miocene Lake Sinj sequences (Mandic et al., 2008) and the Middle-Upper Miocene limestones from the Teruel basin (Ezquerro, 2017). The gastropod biofacies in Holocene vegetated lakes and ponds of the Pampean region (Argentina) may represent good modern analogues of the studied Miocene gastropod-rich deposits (Cristini and De Francesco, 2012; Stutz et al., 2014). A second but minor type of gastropod accumulation corresponds to coquina layers interspersed within both the massive and layered bioclastic limestones. They are thin (<1 cm) and laterally-discontinuous shelly concentrations of packstone-grainstone texture made of similar amounts of entire shells and shell fragments. These accumulations clearly represent a reworked thanatocenosis associated to storm activity or episodes of moderate to high-energy. By contrast, relatively thick and extensive mollusc coquinas are very common in lacustrine systems with moderate to high-energy littoral zones evolving under persistent winds and/or frequent storm activity. The best documented recent to modern examples occur in the large lakes along the east African rift system (Tanganyka, Malawi, Turkana), with numerous examples of gastropod-bivalve coquinas forming bioclastic beach face accumulations, proximal offshore bars and storm beds (i.e. Cohen, 1989; Ring and Betzler, 1995; McGlue et al., 2010). Similar deposits are infrequent or absent in small shallow lakes such as the Peña Adrian system due to the limited fetch for wind activity

and the baffling role of extensive aquatic plants.

6. Conclusions

The Upper Miocene Peña Adrian Formation documents the last filling stage of the piggy-back Miranda-Trebiño basin, through an up to 50–160 m thick clastic and carbonate rock succession that lies unconformably on Cretaceous to Oligocene series. Thirteen sedimentary facies are characterized. These are grouped into four main facies associations that represent alluvial (FA1), open lacustrine (FA2), palustrine (FA3) and restrictive lacustrine (FA4) depositional environments. A low-energy shallow freshwater lake with ramp-shaped margins and extensive palustrine fringes is envisaged for deposition of FAs 2 and 3. The lake experienced water level changes, which could drop to evaporative conditions, as embodied by FA4. The $\delta^{13}C$ and $\delta^{18}O$ values of the carbonate facies reflected changes in biological CO_2 input and Precipitation/Evaporation rates which correlated with distinct depositional and hydrological conditions, consistent with the aforementioned environments.

The enhanced production of biogenic carbonate sediment, as exemplified by rich and varied assemblages of gastropods, charophyte and ostracods, allows to interpret a lake ecosystem with well-oxygenated and slightly alkaline waters under varied nutrient levels. The good preservation of carbonate bioclasts, including gastropods with aragonitic and bimineralic shells, in most open lacustrine deposits, likely indicates rapid burial and reduced degradation. By contrast, bad fossil preservation in the palustrine facies is probably related to early diagenetic pathways in marginal and shallow littoral areas.

Overall, the Peña Adrian lacustrine system embodies a complete cycle of gradual lake expansion, from an initial dominant palustrine area that subsequently evolved to open lacustrine conditions, followed by a comparatively shorter lake retreat and final fill characterized by a broad palustrine setting. The $\delta^{13}C$ and $\delta^{18}O$ smooth trend through time is consistent with this interpretation. This large-scale cycle was punctuated by shorter cycles of water level change, consisting of sharp-based m-thick facies sequences, which are best recorded in the open lacustrine domain. These depositional cycles could match with short climate changes detected in continental records in western Europe during the Late Miocene, which in some cases have been linked to precession and short-term eccentricity cycles. To what extent such cycles are recorded in the Peña Adrian system is difficult to ascertain due to the lack of good chronostratigraphic constraints but, in any case, open a line of research to be confirmed or ruled out in the near future.

Supplementary data to this article can be found online at https://doi.org/10.1016/j.sedgeo.2025.106899.

CRediT authorship contribution statement

Zuriñe Larena: Writing – original draft, Validation, Supervision, Investigation. **Concha Arenas:** Writing – original draft, Investigation. **Josep Sanjuan:** Investigation. **Ana Pascual:** Methodology, Investigation. **Mariano Larraz:** Investigation. **Xabier Murelaga:** Investigation. **Juan Ignacio Baceta:** Writing – original draft, Supervision, Investigation.

Declaration of competing interest

The authors declare that they have no known competing financial interests or personal relationships that could have appeared to influence the work reported in this paper.

Acknowledgements

This research was supported by a pre-Doctoral research grant from the University of the Basque Country (UPV/EHU) as part of Z.L. PhD research. Is a contribution to the Consolidate Research Group IT-1602-22 of the Basque Government University Research System. CA received financial support from GeoTransfer Group. Dr. F.J. Pérez-Rivarés is thanked for his help with statistical treatment of isotopic data. Our gratitude to editor Dr. Catherine Chagué and reviewers Dr. Marcello G. Simões and anonymous reviewer for their helpful revision notes and comments.

Data availability

No data was used for the research described in the article.

References

Abdul Aziz, H., Hilgen, F., Krijgsman, W., Sanz, E., Calvo, J.P., 2000. Astronomical forcing of sedimentary cycles in the middle to late Miocene continental Calatayud Basin (NE Spain). Earth and Planetary Science Letters 177, 9–22. https://doi.org/10.1016/S0012-821X(00)00035-2.

Abels, H.A., Abdul Aziz, H., Ventra, D., Hilgen, F., 2009. Orbital climate forcing in mudflat to marginal lacustrine deposits in the Miocene Teruel basin (Northeast Spain). Journal of Sedimentary Research 79, 831–847. https://doi.org/10.2110/jsr.2009.081.

Alonso-Zarza, A.M., 2003. Palaeoenvironmental significance of palustrine carbonates and calcretes in the geological record. Earth Science Reviews 60, 261–298. https://doi.org/10.1016/S0012-8252(02)00106-X.

Alonso-Zarza, A.M., Wright, V.P., 2010. Palustrine carbonates. In: Alonso-Zarza, A.M., Tanner, L.H. (Eds.), Carbonates in Continental Settings: Facies, Environments and Processes, Developments in Sedimentology, vol. 61. Elsevier, Amsterdam, pp. 103–132.

Alonso-Zarza, A.M., Calvo, J.P., García del Cura, M.A., 1992. Palustrine sedimentation and associated features—grainification and pseudo-microkarst—in the Middle Miocene (intermediate unit) of the Madrid Basin, Spain. Sedimentary Geology 76, 43–61.

Alonso-Zarza, A.M., Sancho, R., Calvo, J.P., 2002. El terciario continental del sector Alfambra-Villalba Alta, fosa de Teruel. Geogaceta 32, 255–258.

Alonso-Zarza, A.M., Meléndez, A., Martín-García, R., Herrero, M.J., Martín-Pérez, A., 2012. Discriminating between tectonism and climate signatures in palustrine deposits: lessons from the Miocene of the Teruel Graben, NE Spain. Earth Science Reviews 113, 141–160. https://doi.org/10.1016/j.earscirev.2012.03.011.

Álvarez-Halcón, R.M., Oscoz, J., Larraz, M.L., 2012. Guía de campo. Moluscos Acuáticos de la Cuenca del Ebro. Confederación Hidrográfica del Ebro, Zaragoza, pp. 1–147.

Anadón, P., Robles, F., Roca, E., Utrilla, R., Vázquez, A., 1998. Lacustrine sedimentation in the diapir-controlled Miocene Bicorb Basin, eastern Spain. Palaeogeography, Palaeoclimatology, Palaeoecology 140, 217–243. https://doi.org/10.1016/S0031-0182(98)00045-5.

Arenas, C., Pardo, G., 1999. Latest Oligocene-Late Miocene lacustrine systems of the north-central part of the Ebro Basin (Spain): sedimentary facies model and palaeogeographic synthesis. Palaeogeography, Palaeoclimatology, Palaeoecology 151, 127–148. https://doi.org/10.1016/S0031-0182(99)00025-5.

Arenas, C., Casanova, J., Pardo, G., 1997. Stable-isotope characterization of the Miocene lacustrine systems of Los Monegros (Ebro Basin, Spain): palaeogeographic and palaeoclimatic implications. Palaeogeography, Palaeoclimatology, Palaeoecology 128, 133–155. https://doi.org/10.1016/S0031-0182(96)00052-1.

Arenas, C., Osácar, O., Pérez-Rivarés, F.J., Bastida, J., Gil, A., Auqué, L.F., 2024. The early–middle Miocene climate as reflected by a mid-latitude lacustrine record in the Ebro basin, north-east Iberia. The Depositional Record 00, 1–26. https://doi.org/10.1002/dep2.290.

Armenteros, I., 1991. Contribución al conocimiento del Mioceno lacustre de la cuenca terciaria del Duero (sector centro-oriental, Valladolid-Penafiel-Sacramenia-Cuéllar). Acta Geologica Hispánica 26 (2), 97–131 (in Spanish with English abstract).

Armenteros, I., 2010. Diagenesis of carbonates in continental settings. In: Alonso-Zarza, A.M., Tanner, L.H. (Eds.), Carbonates in Continental Settings: Geochemistry, Diagenesis and Applications, Developments in Sedimentology, vol. 62. Elsevier, Amsterdam, pp. 61–151.

Armenteros, I., Daley, B., 1998. Pedogenic modification and structure evolution in palustrine facies as exemplified by the Bembridge limestones (Upper Eocene) of the Isle of Wight, southern England. Sedimentary Geology 119, 275–295.

Armenteros, I., Daley, B., García, E., 1997. Lacustrine and palustrine facies in the Bembridge Limestone (late Eocene, Hamshire Basin) of Isle of Wight, southern England. Palaeogeography, Palaeoclimatology, Palaeoecology 128, 111–132. https://doi.org/10.1016/S0031-0182(96)00108-3.

Arostegui, J., Baceta, J.I., Pujalte, V., Carracedo, M., 2011. Late Cretaceous-Palaeocene mid-latitude climates: inferences from clay mineralogy of continental-coastal sequences (Tremp-Graus area, southern Pyrenees, N Spain). Clay Minerals 46, 105–126. https://doi.org/10.1180/claymin.2011.046.1.105.

Benavente, C.A., Bohacs, K.M., 2024. Advances in limnogeology: the lake-basin-type model revisited 25 years after…anomalies, conundrums and upgrades. The Depositional Record 10 (5), 748–792. https://doi.org/10.1002/dep2.280.

Bohacs, K.M., Carroll, A.R., Neal, J.E., Mankiewicz, P.J., 2000. Lake-basin type, source potential, and hydrocarbon character: an integrated sequence stratigraphic-geochemical framework. In: Gierlowski-Kordesch, E.H., Kelts, K. (Eds.), Lake Basins Through Space and Time, Studies in Geology, vol. 46. American Association of Petroleum Geologists, pp. 3–34.

Böhme, M., Ilg, A., Winklhofer, M., 2008. Late Miocene "washhouse" climate in Europe. Earth and Planetary Science Letters 275, 393–401. https://doi.org/10.1016/j.epsl.2008.09.011.

Böhme, M., Winklhoferb, M., Ilgc, A., 2011. Miocene precipitation in Europe: temporal trends and spatial gradients. Palaeogeography, Palaeoclimatology, Palaeoecology 304, 212–218. https://doi.org/10.1016/j.palaeo.2010.09.028.

Bustillo, M.A., 2010. Silicification of continental carbonates. In: Alonso-Zarza, A.M., Tanner, L.H. (Eds.), Carbonates in Continental Settings: Processes, Facies and Applications, Developments in Sedimentology, vol. 62. Elsevier, Oxford, pp. 153–174.

Bustillo, M.A., Arribas, M.E., Bustillo, M., 2002. Dolomitization and silicification in low energy lacustrine carbonates (Paleogene, Madrid Basin, Spain). Sedimentary Geology 151 (1–2), 107–126. https://doi.org/10.1016/S0037-0738(01)00234-2.

Cabrera, L.I., Sáez, A., 1987. Coal deposition in carbonate-rich shallow lacustrine systems: the Calaf and Mequinenza sequences (Oligocene, eastern Ebro Basin, NE Spain). Journal of the Geological Society of London 144, 451–461. https://doi.org/10.1144/gsjgs.144.3.0451.

Calvo, J.P., Jones, B.F., Bustillo, M., Fort, R., Alonso-Zarza, A.M., Kendall, C., 1995. Sedimentology and geochemistry of carbonates from lacustrine sequences in the Madrid Basin, Central Spain. Chemical Geology 123, 173–191.

Cañaveras, J.C., Calvo, J.P., Ordóñez, S., Muñoz-Cervera, M.C., Sánchez-Moral, S., 2020. Tectono-sedimentary evolution of the Madrid Basin paleokarst (Spain) during the Late Miocene: data from profiles in diagenetically-complex continental carbonates. Geosciences 10, 433. https://doi.org/10.3390/geosciences10110433.

Carlotto, M.A., Da Silva, R.C.B., Yamato, A.A., 2017. Libra: a newborn giant in the Brazilian presalt province. In: Merrill, R.K., Sternbach, C.A. (Eds.), Giant Fields of the Decade 2000–2010, AAPG Memoir, vol. 113, pp. 165–176. https://doi.org/10.1306/13572006M1133685.

Carroll, A.R., Bohacs, K.M., 1999. Stratigraphic classification of ancient lakes: balancing tectonic and climatic controls. Geology 27, 99–102. https://doi.org/10.1130/0091-7613(1999)027<0099:SCOALB>2.3.CO;2.

Carvalho, M.D., Praça, U.M., Silva-Telles Jr., A.C., Jahnert, R.J., Dias, J.L., 2000. Bioclastic carbonate lacustrine facies models in the Campos Basin (Lower Cretaceous), Brazil. In: Gierlowski-Kordesch, E.H., Kelts, K.R. (Eds.), Lake Basins Through Space and Time, AAPG Studies in Geology, vol. 46. AAPG, Tulsa, Oklahoma, USA, pp. 245–256.

Casanova, M.T., García, A., Feist, M., 2003. The ecology and conservation of Lychnothamnus barbatus (Characeae). Acta Microbiologica Sinica 20 (2), 118–128.

Cherns, L., Wright, V.P., 2011. Skeletal mineralogy and biodiversity of marine invertebrates: size matters more than seawater chemistry. Geological Society of London, Special Publication 358, 9–17. https://doi.org/10.1144/SP358.2.

Cohen, A.S., 1989. Facies relationships and sedimentation in large rift lakes and implications for hydrocarbon exploration: examples from lakes Turkana and Tanganyika. Palaeogeography, Palaeoclimatology, Palaeoecology 70, 65–80. https://doi.org/10.1016/0031-0182(89)90080-1.

Cortés-Gracia, A.L., Casas-Sainz, A.M., 1997. Fosas neógenas asociadas a reactivación de pliegues en el borde sur de la Sierra de Cantabria (Alava-Navarra). Geogaceta 21, 81–84 (in Spanish with English abstract).

Costa, E., Garcés, M., López-Blanco, M., Beamud, E., Gómez-Paccard, M., Larrasoaña, J. C., 2010. Closing and continentalization of the South Pyrenean foreland basin (NE Spain): magnetochronological constraints. Basin Research 22, 904–917. https://doi.org/10.1111/j.1365-2117.2009.00452.x.

Cristini, P.A., De Francesco, C.G., 2012. Análisis tafonómico de moluscos por debajo de la interfase agua-sedimento en la laguna Nahuel Rucá (provincia de Buenos Aires, Argentina). Ameghiniana 49 (4), 594–605 (in Spanish with abstract in English).

Davis, S.J., Wiegand, B.A., Carroll, A.R., Chamberlain, C.P.G., 2008. The effect of drainage reorganization on paleoaltimetry studies: an example from the Paleogene Laramide foreland. Earth and Planetary Science Letters 275, 258–268. https://doi.org/10.1016/j.epsl.2008.08.009.

Davó, O., Ramírez del Pozo, J., Riba, O., 1978. Mapa Geológico de España 1:50.000, hoja n° 137 (Miranda de Ebro) y memoria. IGME, Madrid, p. 44 (in Spanish).

De Wet, C., Yocum, D.A., Mora, C., 1998. Carbonate lakes in closed basins: sensitive indicators of climate and tectonics: an example from the Gettysburg Basin (Triassic), Pennsylvania, USA. In: Stanley, K.W., McCabe, P.J. (Eds.), Relative Role of Eustasy, Climate and Tectonism in Continental Rocks, Special Publication, vol. 59. Society of Economic Paleontologists and Mineralogists, pp. 191–209.

Deocampo, D.M., 2010. The geochemistry of continental carbonates. In: Alonso-Zarza, A. M., Tanner, L.H. (Eds.), Carbonates in Continental Settings: Geochemistry, Diagenesis and Applications, Developments in Sedimentology, vol. 62. Elsevier, Amsterdam, pp. 1–59. https://doi.org/10.1016/S0070-4571(09)06201-3.

Dillon, R.T., 2006. Freshwater gastropoda. In: Sturm, C.F., Pearce, T.A., Valdés, A. (Eds.), The Mollusks: A Guide to Their Study, Collection, and Preservation. American Malacological Society, Los Angeles and Pittsburgh, pp. 251–259.

Dunham, R.J., 1962. Classification of carbonate rocks according to depositional texture. In: Ham, W.E. (Ed.), Classification of Carbonate Rocks, Memoir of the American Association of Petroleum Geologists, Tusla, pp. 108–121.

Embry, A.F., Klovan, J.E., 1971. A late Devonian reef tract on northeastern Banks Island, NW Territories. Bulletin of Canadian Petroleum Geology 19, 730–781.

Ezquerro, L., 2017. El sector norte de la cuenca neógena de Teruel: tectónica, clima y sedimentación. Universidad de Zaragoza, Spain (Ph.D. Thesis, 452 pp., in Spanish with English abstract).

Ezquerro, L., Luzón, A., Navarro, M., Liesa, C.L., Simón, J.L., 2014. Climatic vs. tectonic signals in a continental extensional basin (Teruel, NE Spain) from stable isotope ($\delta^{18}O$) and sequence stratigraphical evolution. Terra Nova 26, 337–346. https://doi.org/10.1111/ter.12101.

Ezquerro, L., Muñoz, A., Liesa, C.L., Simón, J.L., Luzón, A., 2022. Late Neogene to Early Quaternary climate evolution in southwestern Europe from a continental perspective. Global and Planetary Change 211, 103788. https://doi.org/10.1016/j.gloplacha.2022.103788.

Flügel, E., 2004. Microfacies and Carbonate Rocks. Analysis, Interpretation and Application. Springer Berlin Heidelberg, Berlin, Heidelberg, p. 984. https://doi.org/10.1007/978-3-662-08726-8.

Frankovic, A., Eguiluz, L., Martínez-Torres, L.M., 2016. Geodynamic evolution of the Salinas de Añana diapir in the Basque-Cantabrian Basin, Western Pyrenees. Journal of Structural Geology 83, 13–27. https://doi.org/10.1016/j.jsg.2015.12.001.

Freytet, P., 1973. Petrography and paleo-environment of continental carbonate deposits with particular reference to the Upper Cretaceous and Lower Eocene of Languedoc (southern France). Sedimentary Geology 10, 25–60.

Freytet, P., Plaziat, J.C., 1982. Continental carbonate sedimentation and pedogenesis. Late cretaceous and early Tertiary of Southern France. In: Purser, B.H. (Ed.), Contributions to Sedimentology, vol. 12. Schweizerbart'sche Verlag, Stuttgart, Germany. https://www.worldcat.org/title/455909843 (217 pp.).

Freytet, P., Verrechia, E.P., 2002. Lacustrine and palustrine carbonate petrography: an overview. Journal of Paleolimnology 27, 221–237. https://doi.org/10.1023/A:1014263722766.

Friend, P.F., Dabrio, C.J., 1996. Tertiary basins of Spain the stratigraphic record of crustal kinematics. In: Friend, P.F., Dabrio, C.J. (Eds.), World and Regional Geology Series, vol. 6. Cambridge University Press, Cambridge (400 pp.).

Garcés, M., López-Blanco, M., Valero, L., Beamud, E., Muñoz, J.A., Oliva-Urcia, B., Vinyoles, A., Arbués, P., Cabello, P., Cabrera, L., 2020. Paleogeographic and sedimentary evolution of the South Pyrenean foreland basin. Marine and Petroleum Geology 113, 104105. https://doi.org/10.1016/j.marpetgeo.2019.104105.

García del Cura, M.A., Calvo, J.P., Ordoñez, S., Jones, B.F., Cañaveras, J.C., 2001. Petrographic and geochemical evidence for the formation of primary, bacterially induced lacustrine dolomite: La Roda `white earth' (Pliocene, central Spain). Sedimentology 48, 897–915.

Gierlowski-Kordesch, E.H., 2010. Lacustrine carbonates. In: Alonso-Zarza, A.M., Tanner, L.H. (Eds.), Lacustrine Carbonates, Developments in Sedimentology, vol. 61. Elsevier, Amsterdam, pp. 1–101. https://doi.org/10.1016/S0070-4571(09)06101-9.

Glenn, C.R., Kelts, K., 1991. Sedimentary rhythms in lake deposits. In: Einsele, G., Ricken, W., Seilacher, A. (Eds.), Cycles and Events in Stratigraphy. Springer-Verlag, New York, pp. 188–221.

Hammer, Ø., Harper, D.A.T., Ryan, P.D., 2001. PAST: paleontological statistics software package for education and data analysis. Palaeontologia Electronica 4 (1), 1–9.

Hassan, H., Adams, N., Billing, I., 2016. Depositional setting and facies geometry of lacustrine coquina reservoirs: examples from the west African margin. In: International Conference and Exhibition, Barcelona. https://doi.org/10.1190/ice2016-6508978.1 (46 p.).

Hogan, P.J., Burbank, D.W., 1996. Evolution of the Jaca piggyback basin and emergence of the External Sierras, Southern Pyrenees. In: Friend, P.F., Dabrio, C.J. (Eds.), Tertiary Basins of Spain: The Stratigraphic Record of Crustal Kinematics. Cambridge University Press, Cambridge, pp. 153–160.

Horita, J., 2014. Oxygen and carbon isotope fractionation in the system dolomite-water-CO_2 to elevated temperatures. Geochimica et Cosmochimica Acta 129, 111–124. https://doi.org/10.1016/j.gca.2013.12.027.

Huerta, P., 2006. Paleógeno de la Cuenca de Almazán: relleno de una cuenca piggyback. Universidad de Salamanca, Spain (Ph.D. Thesis, 150 pp., in Spanish with English abstract).

Jahnert, R., Paula, O., Collins, L., Strobach, E., Pevzner, R., 2012. Evolution of a coquina barrier in Shark Bay, Australia by GPR imaging: architecture of a Holocene reservoir analogue. Sedimentary Geology 281, 59–74. https://doi.org/10.1016/j.sedgeo.2012.08.009.

Jiménez-Moreno, G., Fauquette, S., Suc, J.P., 2010. Miocene to Pliocene vegetation reconstruction and climate estimates in the Iberian Peninsula from pollen data. Review of Palaeobotany and Palynology 162 (3), 403–415. https://doi.org/10.1016/j.revpalbo.2009.08.001.

Kelts, K., Talbot, M., 1990. Lacustrine carbonates as geochemical archives of environmental change and biotic-abiotic interactions. In: Tilzer, M.M., Serruya, C. (Eds.), Large Lakes: Ecological Structure and Function. Springer-Verlag, Berlin, pp. 288–315. https://doi.org/10.1007/978-3-642-84077-7_15.

Kim, S.-T., O'Neil, J.R., Hillaire-Marcel, C., Mucci, A., 2007. Oxygen isotope fractionation between synthetic aragonite and water: influence of temperature and Mg^{2+} concentration. Geochimica et Cosmochimica Acta 71, 4704–4715. https://doi.org/10.1016/j.gca.2007.04.019.

Kinoshita, E.M., 2010. Modelagem sísmica-geométrica de fácies dos carbonatos lacustres da Formação Morro do Chaves, Bacia de Sergipe-Alagoas. Boletim de Geociencias da Petrobras 18, 249–269. Rio de Janeiro, in Portugues.

Krause, W., 1997. Charales. In: Ettl, H., Gärtner, G., Heynig, H., Mollenhauer, D. (Eds.), Süßwasserflora von Mitteleuropa, vol. 18. Gustav Fischer Verlag, Stuttgart (202 pp.).

Lachniet, M.S., 2009. Climatic and environmental controls on speleothem oxygen-isotope values. Quaternary Science Reviews 28, 412–432. https://doi.org/10.1016/j.quascirev.2008.10.021.

Larena, Z., Sanjuan, J., Pascual, A., Larraz, M., Valenzuela, A., Arenas, C., Murelaga, X., Baceta, J.I., 2023. Estudio paleontológico de las facies lacustres-palustres de Peña Adrián, Mioceno Superior (Miranda de Ebro, Cuenca Miranda-Trebiño). Geogaceta 74, 83–86. https://doi.org/10.55407/geogaceta95534 (in Spanish with English abstract).

Larena, Z., Murelaga, X., Sanjuan, J., Ruiz, F.J., Baceta, J.I., 2024. The middle-upper Eocene Loza-Portilla Formation (Western Pyrenees, North Spain): palustrine-lacustrine carbonate-dominated sequences in a piggy-back basin under

compressional tectonic stress. The Depositional Record 00, 1–28. https://doi.org/10.1002/dep2.298.
Leng, M.J., Marshall, J.D., 2004. Palaeoclimate interpretation of stable isotope data from lake sediment archives. Quaternary Science Reviews 23, 811–831. https://doi.org/10.1016/j.quascirev.2003.06.012.
Mandic, O., Pavelić, D., Harzhauser, M., Zupanič, Reischenbacher, D., Sachsenhofer, R. F., Tadej, N., Vranjković, A., 2008. Depositional history of the Miocene Lake Sinj (Dinaride Lake System, Croatia): a long-lived hard-water lake in a pull-apart tectonic setting. Journal of Paleolimnology 41 (3), 431–452. https://doi.org/10.1007/s10933-008-9235-1.
Martín-Alafont, J.M., Ramírez del Pozo, J., Portero, J.M., 1978. Mapa Geológico de España 1:50.000, hoja n° 138 (Puebla de Arganzón) y memoria. IGME, Madrid, p. 46 (in Spanish).
Martín-Closas, C., Wojcicki, J.J., Fonollá, L., 2006. Fossil charophytes and hydrophytic angiosperms as indicators of lacustrine trophic change. A case study in the Miocene of Catalonia (Spain). Cryptogamie Algologie 27, 357–379.
Martín-Rubio, M., 2003. Ostrácodos del Plioceno y Reciente en el sector occidental de la Cuenca del Ebro: Paleoecología y Geoquímica. University of the Basque Country, Spain (Unpublished Ph.D. thesis, 312 pp., in Spanish).
McCrea, J., 1950. On the isotopic chemistry of carbonates and a paleotemperature scale. The Journal of Chemical Physics 18 (6), 849–857. https://doi.org/10.1063/1.1747785.
McGlue, M.M., Soreghan, M.J., Michel, E., Todd, J.A., Cohen, A.S., Mischler, J., Nkotagu, H.H., 2010. Environmental controls on shell-rich facies in tropical lacustrine rifts: a view from Lake Tanganyika's littoral. PALAIOS 25, 426–438. https://doi.org/10.2110/palo.2009.p09-160r.
Meisch, C., 2000. Freshwater Ostracoda of Western and Central Europe. Spektrum Akademischer Verlag, Berlin, pp. 1–523.
Miall, A.D., 1996. The Geology of Fluvial Deposits. Springer-Verlag, Berlin, Heidelberg (582 pp.).
Miller, J.P., Delicado, D., García-Guerrero, F., Ramos, M.A., 2022. Recurrent founder-event speciation across the Mediterranean likely shaped the species diversity and geographic distribution of the freshwater snail genus *Mercuria* Boeters, 1971 (Caenogastropoda: Hydrobiidae). Molecular Phylogenetics and Evolution 173, 107524. https://doi.org/10.1016/j.ympev.2022.107524.
Mirumbrales-Ayllón, S., Casas-Sainz, A.M., Román-Berdiel, T., 2023. Los montes Obarenes: diapirismo e inversión tectónica en el margen sur de la cuenca vasco-cantábrica. Revista de la Sociedad Geológica de España 36 (2), 30–45 (in Spanish with English abstract). 10.55407/rsge.99970.
Moreau, K., Andrieu, S., Briais, J., Brigaud, B., Ader, M., 2023. Facies distribution and depositional cycles in lacustrine and palustrine carbonates: the Lutetian–Aquitanian record in the Paris Basin. The Depositional Record 10 (1), 124–158. https://doi.org/10.1002/dep2.264.
Muniz, M.C., 2013. Tectono-stratigraphic Evolution of the Barremian-Aptian Continental Rift Carbonates in Southern Campos Basin, Brazil. Royal Holloway University of London (Ph.D. Thesis, 343 pp.).
Muñoz, J.A., 2002. The Pyrenees. In: Gibbons, W., Moreno, T. (Eds.), The Geology of Spain. The Geological Society of London, London, pp. 370–385.
Muñoz, J.A., 2019. Alpine Orogeny: Deformation and Structure in the Northern Iberian Margin (Pyrenees s.l). In: Quesada, C., Oliveira, J. (Eds.), The Geology of Iberia: A Geodynamic Approach, Regional Geology Reviews. Springer, Cham, pp. 433–451. https://doi.org/10.1007/978-3-030-11295-0_9.
Murray, S.T., Swart, P.K., 2017. Evaluating formation fluid models and calibrations using clumped isotope paleothermometry on Bahamian dolomites. Geochimica et Cosmochimica Acta 206, 73–93. https://doi.org/10.1016/j.gca.2017.02.021.
Neubauer, T.A., 2024. The fossil record of freshwater Gastropoda – aglobal review. Biological Reviews 99, 177–199. https://doi.org/10.1111/brv.13016.
Ninemets, E., 1999. Lake Peipsi: paleoecological and Paleoclimatic Interpretations on Ostracod Data. University of Tartu (Master Thesis, 66 pp.).
Oliveira, V.C.B., Silva, C.M.A., Borghi, L.F., Carvalho, I.S.I., 2019. Lacustrine coquinas and hybrid deposits from rift phase. Pre-Salt, lower cretaceous, Campos Basin, Brazil. Journal of South American Earth Sciences 95, 102254. https://doi.org/10.1016/j.jsames.2019.102254.
Ortiz, A., Guillocheau, F., Lasseur, E., Briais, J., Robin, C., Serrano, O., Fillon, C., 2020. Sediment routing system and sink preservation during the post-orogenic evolution of a retro-foreland basin: the case example of the North Pyrenean (Aquitaine, Bay of Biscay) Basins. Marine and Petroleum Geology 112, 104085. https://doi.org/10.1016/j.marpetgeo.2019.104085.
Paredes, J.M., Foix, N., Colombo Piñol, F., Nillni, A., Allard, J.O., Marquillas, R.A., 2007. Volcanic and climatic controls on fluvial style in a high-energy system: the Lower Cretaceous Matasiete Formation, Golfo San Jorge Basin, Argentina. Sedimentary Geology 202, 96–123. https://doi.org/10.1016/j.sedgeo.2007.05.007.
Platt, N.H., 1989. Lacustrine carbonates and pedogenesis: sedimentology and origin of palustrine deposits from the Early Cretaceous Rupelo Formation, W Cameros Basin, N Spain. Sedimentology 36, 665–684. https://doi.org/10.1111/j.1365-3091.1989.tb02092.x.
Platt, N.H., Wright, V.P., 1991. Lacustrine carbonates: facies models, facies distributions and hydrocarbons aspects. In: Anadón, P., Cabrera, L., Kelts, K. (Eds.), Lacustrine Facies Analysis, Special Publication of the International Association of Sedimentologists, vol. 13. Blackwell, Oxford, UK, pp. 57–74. https://doi.org/10.1002/9781444303919.ch3.
Platt, N.H., Wright, V.P., 1992. Palustrine carbonates and the Florida Everglades: towards an exposure index for the freshwater environment. Journal of Sedimentary Petrology 62, 1058–1071. https://doi.org/10.1306/D4267A4B-2B26-11D7-8648000102C1865D.
Platt, N.H., Wright, V.P., 2024. Hydrologically sensitive carbonates: tectonic and groundwater controls on synrift sedimentation in the late Jurassic–early Cretaceous of the western Cameros Basin, Northern Spain. The Depositional Record 00, 1–28. https://doi.org/10.1002/dep2.317.
Plaziat, J.C., 1981. Late Cretaceous to Late Eocene palaeogeographic evolution of southwest Europe. Palaeogeography, Palaeoclimatology, Palaeoecology 36, 263–320. https://doi.org/10.1016/0031-0182(81)90110-3.
Portero García, J.M., Ramírez del Pozo, J., Aguilar Tomás, M.J., 1976. Mapa Geológico de España 1:50.000, hoja n° 169 (Casalarreina) y memoria. IGME, Madrid (41 p., in Spanish).
Pujalte, V., Baceta, J.I., Payros, A., 2002. Tertiary: western Pyrenees and Basque–Cantabrian region. In: Gibbons, W., Moreno, T. (Eds.), The Geology of Spain. Geological Society of London, London, pp. 293–301.
Riba, O., 1956. La Cuenca Terciaria de Miranda Treviño. Informe inédito. CIEPSA (28 p., in Spanish).
Riba, O., 1961. Nuevas observaciones sobre el Terciario continental de la Cuenca de Miranda Treviño. Informe inédito CIEPSA (19 p., in Spanish).
Riba, O., Jurado, M.J., 1992. Reflexiones sobre la geología occidental de la Depresión del Ebro. Acta Geologica Hispánica 27, 177–193 (in Spanish with English abstract).
Ring, U., Betzler, C., 1995. Geology of the Malawi Rift: kinematic and tectonosedimentary background to the Chiwondo Beds, northern Malawi. Journal of Human Evolution 28 (1), 7–21. https://doi.org/10.1006/jhev.1995.1003.
Rodríguez-Aranda, J.P., Calvo, J.P., 1998. Trace fossils and rhizoliths as a tool for sedimentological and palaeoenvironmental analysis of ancient continental evaporite successions. Palaeogeography, Palaeoclimatology, Palaeoecology 140, 383–399. https://doi.org/10.1016/S0031-0182(98)00036-4.
Romanek, C., Grossman, E.L., Morse, J.W., 1992. Carbon isotopic fractionation in synthetic aragonite and calcite: Effects of temperature and precipitation rate. Geochimica et Cosmochimica Acta 56 (1), 419–430. https://doi.org/10.1016/0016-7037(92)90142-6.
Sáez, A., Valero-Garcés, B.L., Moreno, A., Bao, R., Pueyo, J.J., González-Sampériz, P., Giralt, S., Taberner, C., Herrera, C., Gibert, R.O., 2007. Lacustrine sedimentation in active volcanic settings: the Late Quaternary depositional evolution of Lake Chungará (northern Chile). Sedimentology 54, 1191–1222.
Sanders, D., 2003. Syndepositional dissolution of calcium carbonate in neritic carbonate environments: geological recognition, processes, potential significance. Journal of African Earth Sciences 36 (3), 99–134.
Sanjuan, J., Matamoros, D., Casanovas-Vilar, I., Vicente, A., Moreno-Bedmar, J.A., Martín-Closas, C., 2022. Palaeoecology of Middle Miocene charophytes from the Vallès–Penedès and Vilanova basins (Catalonia, Spain). Historical Biology 36, 1665–1685. https://doi.org/10.1080/08912963.2022.2106861.
Sanz, M.E., 1994. Sedimentología de las formaciones neógenas del sur de la Cuenca de Madrid, con énfasis en los procesos kársticos asociados a las rupturas sedimentarias del Plioceno. Universidad Complutense de Madrid, Spain (Ph.D. Thesis, 333 pp., in Spanish).
Scott, J.J., Smith, M.E., 2015. Trace fossils of the Eocene Green River Lake Basins, Wyoming, Utah and Colorado. In: Smith, M.E., Carroll, A.R. (Eds.), Stratigraphy and Paleolimnology of the Green River Formation, Western USA, Syntheses in Limnogeology, vol. 1. Springer Science and Business Media, Dordrecht, pp. 313–350.
Shevenell, A.E., Kennett, J.P., Lea, D.W., 2004. Middle Miocene southern ocean cooling and Antarctic cryosphere expansion. Science 305, 1766–1770. https://doi.org/10.1126/science.1100061.
Sommer, M., Kaczorek, D., Kuzyakov, Y., Breuer, J., 2006. Silicon pools and fluxes in soils and landscapes—a review. Z. Journal of Plant Nutrition and Soil Science 169 (3), 310–329. https://doi.org/10.1002/jpln.200521981.
Soulié-Märsche, I., 1989. Etude comparée de gyrogonites de Charophytes actuelles et fossiles et phylogénie des genres actuels. Imprimerie des Tilleuls, Millau, France (237 pp., in French).
Sreenivasan, S.P., Bera, M.K., Samanta, A., 2023. A simple but improved protocol for measuring carbon and oxygen isotope ratios of calcite in calcite-dolomite mixtures. Applied Geochemistry 150, 105600. https://doi.org/10.1016/j.apgeochem.2023.105600.
Steenbrink, J., Van Vugt, N., Hilgen, F.J., Wijbrans, J.R., Meulenkamp, J.E., 1999. Sedimentary cycles and volcanic ash beds in the lower Pliocene lacustrine succession of Ptolemais (NW Greece): discrepancy between 40Ar/39Ar and astronomical ages. Palaeogeography, Palaeoclimatology, Palaeoecology 152, 283–303.
Steinthorsdottir, M., Coxall, H.K., de Boer, A.M., Huber, M., Barbolini, N., Bradshaw, C. D., Burls, N.J., Feakins, S.J., Gasson, E., Henderiks, J., Holbourn, A.E., Kiel, S., Kohn, M.J., Knorr, G., Kürschner, W.M., Lear, C.H., Liebrand, D., Lunt, D.J., Mörs, T., Pearson, P.N., Pound, M.J., Stoll, H., Strömberg, C.A.E., 2020. The Miocene: the future of the past. Paleoceanography and Paleoclimatology 36, e2020PA004037. https://doi.org/10.1029/2020PA004037.
Straub, E.W., 1952. Mikropalaöntologische Untersuchungen im Tertiär zwischen Ehingen und Ulm an der Donau. Geologisches Jahrbuch 66, 433–524 (in German).
Sturm, M., Matter, A., 1978. Turbidites and varves in Lake Brienz (Switzerland): deposition of clastic detritus by density currents. Special Publications of the International Association of Sedimentologist 2, 147–168.
Stutz, S., Tonello, M.S., González Sagrario, M.A., Navarro, D., Fontana, S.L., 2014. Historia ambiental de los lagos someros de la llanura pampeana (Argentina) desde el Holoceno Medio: inferencias paleoclimáticas. Latin American Journal of Sedimentology and Basin Análisis 21 (2), 119–138 (in Spanish with abstract in English).
Talbot, M.R., 1990. A review of the palaeohydrological interpretation of carbon and oxygen isotopic ratios in primary lacustrine carbonates. Chemical Geology: Isotope Geoscience 80, 261–279. https://doi.org/10.1016/0168-9622(90)90009-2.

Tanner, L.H., 2000. Palustrine–lacustrine and alluvial facies of the (Norian) owl rock formation (Chinle group), four corners region, southwestern U.S.A: implications for late Triassic paleoclimate. Journal of Sedimentary Research 70 (6), 1280–1289. https://doi.org/10.1306/031700701280.

Tavares, A.C., Borghi, L., Corbett, P., Nobre-Lopes, J., Camara, R., 2015. Facies and depositional environments for the coquinas of the Morro do Chaves Formation, Sergipe Alagoas Basin, defined by taphonomic and compositional criteria. Brazilian Journal of Genetics 45 (3), 415–429. https://doi.org/10.1590/2317-488920150030211.

Teixell, A., Labaume, P., Lagabrielle, Y., 2016. The crustal evolution of the west-central Pyrenees revisited: inferences from a new kinematic scenario. Comptes Rendus Geoscience 348, 257–267. https://doi.org/10.1016/j.crte.2015.10.010.

Teixell, A., Labaume, P., Ayarza, P., Espurt, N., de Saint Blanquat, M., Lagabrielle, Y., 2018. Crustal structure and evolution of the Pyrenean-Cantabrian belt: a review and new interpretations from recent concepts and data. Tectonophysics 724–725, 146–170. https://doi.org/10.1016/j.tecto.2018.01.009.

Tessier, C., Cattaneo, A., Pinel-Alloul, B., Galanti, G., Morabito, G., 2004. Biomass, composition and size structure of invertebrate communities associated to different types of aquatic vegetation during summer in Lago di Candia (Italy). Journal of Limnology 63, 190–198. https://doi.org/10.4081/JLIMNOL.2004.190.

Thompson, D.L., Jeffrey, D.S., Halla, M., 2015. Lacustrine carbonate reservoirs from Early Cretaceous rift lakes of Western Gondwana: Pre-Salt coquinas of Brazil and West Africa. Gondwana Research 28, 26–51. https://doi.org/10.1016/j.gr.2014.12.005.

Torromé, D., Aurell, M., Martín-Pérez, A., Košir, A., 2023. A carbonate palustrine system with marshes and shallow ephemeral lakes (Campanian, northeastern Iberian Basin). Sedimentary Geology 456, 106516. https://doi.org/10.1016/j.sedgeo.2023.106516.

Tucker, M.E., Wright, V.P., 1990. Carbonate Sedimentology. Blackwell, Oxford. https://doi.org/10.1002/9781444314175 (482 p.).

Valenzuela, A., Larena, Z., Murelaga, X., Baceta, J.I., 2023. The oko limestones: a late Miocene-Pliocene fluvial to palustrine carbonate wetland enclosed in the South-Pyrenean thrust front (Navarre, Spain). Geogaceta 74, 7–10.

Valero-Garcés, B.L., Delgado-Huertas, A., Navas, A., Machín, J., González-Sampériz, P., Kelts, K., 2000. Quaternary palaeohydrological evolution of a playa lake: Salada Mediana, central Ebro Basin, Spain. Sedimentology 47, 1135–1156. https://doi.org/10.1046/j.1365-3091.2000.00346.x.

van Dam, J.A., 2006. Geographic and temporal patterns in the late Neogene (12–3 Ma) aridification of Europe: the use of small mammals as paleoprecipitation proxies. Palaeogeography, Palaeoclimatology, Palaeoecology 238, 190–218. https://doi.org/10.1016/j.palaeo.2006.03.025.

Vázquez-Urbez, M., Arenas, C., Pardo, G., Pérez-Rivarés, J., 2013. The effect of drainage reorganization and climate on the sedimentologic evolution of intermontane lake systems: the final fill stage of the Tertiary Ebro basin (Spain). Journal of Sedimentary Research 83, 562–590. https://doi.org/10.2110/jsr.2013.47.

Villalba-Breva, S., Martín-Closas, C., 2013. Upper Cretaceous paleogeography of the Central Southern Pyrenean Basins (Catalonia, Spain) from microfacies analysis and charophyte biostratigraphy. Facies 59, 319–345. https://doi.org/10.1007/s10347-012-0317-1.

Warren, J.K., 2006. Evaporites: Sediments, Resources and Hydrocarbons. Springer, Berlin. https://doi.org/10.1007/3-540-32344-9?nosfx=y (1036 p.).

Wright, V.P., Alonso-Zarza, A., Sanz, M.E., Calvo, J.P., 1997. Diagenesis of late Miocene micritic lacustrine carbonates, Madrid Basin, Spain. Sedimentary Geology 114, 81–95. https://doi.org/10.1016/S0037-0738(97)00059-6.

Wright, V.P., Cherns, L., Azerêdoc, A.C., Cabral, M.C., 2018. Testing whether early diagenesis of skeletal carbonate is different in nonmarine settings: contrasting styles of molluscan preservation in the Upper Jurassic of Portugal. Palaeogeography, Palaeoclimatology, Palaeoecology 492, 1–9. https://doi.org/10.1016/j.palaeo.2017.11.014.

Yui, T.F., Gong, S.Y., 2003. Stoichiometry effect on stable isotope analysis of dolomite. Chemical Geology 201 (3–4), 359–368. https://doi.org/10.1016/j.chemgeo.2003.08.007.

Zachos, J.C., Pagani, M., Sloan, L., Thomas, E., Billups, K., 2001. Trends, rhythms, and aberrations in global climate 65 Ma to present. Science 292, 686–693. https://doi.org/10.1126/science.1059412.